Journal of Organometallic Chemistry 705 (2012) 7–22

Contents lists available at SciVerse ScienceDirect

Journal of Organometallic Chemistry

journal homepage: www.elsevier.com/locate/jorganchem

The preparation, spectroscopy, structure and electrochemistry of some $[Co(\eta^4\text{-}C_4Ph_4)(\eta^5\text{-}C_5H_4C\equiv C{-}CH{=}Y)]$, $[Fe(\eta^5\text{-}C_5H_5)(\eta^5\text{-}C_5H_4C\equiv C{-}CH{=}Y)]$, and related complexes

Donagh Courtney [a], C. John McAdam [b,*], Anthony R. Manning [a], Helge Müller-Bunz [a], Yannick Ortin [a], Jim Simpson [b]

[a] School of Chemistry and Chemical Biology, University College Dublin, Belfield, Dublin 4, Ireland
[b] Department of Chemistry, University of Otago, PO Box 56, Dunedin, New Zealand

ARTICLE INFO

Article history:
Received 23 September 2011
Received in revised form
22 November 2011
Accepted 11 December 2011

Keywords:
Cobalt
Tetraphenylcyclobutadiene
Ferrocenyl
Alkyne
Aldehyde reactions

ABSTRACT

$[Co(\eta^4\text{-}C_4Ph_4)(\eta^5\text{-}C_5H_4C\equiv C{-}CHO)]$, **4a**, has been prepared from $[Co(\eta^4\text{-}C_4Ph_4)(\eta^5\text{-}C_5H_4CHO)]$, **1a**, by reactions similar to those used previously to convert $[Fe(\eta^5\text{-}C_5H_5)(\eta^5\text{-}C_5H_4CHO)]$, **1b**, to $[Fe(\eta^5\text{-}C_5H_5)(\eta^5\text{-}C_5H_4C\equiv C{-}CHO)]$, **4b**, i.e. via the dibromoethene $[Co(\eta^4\text{-}C_4Ph_4)(\eta^5\text{-}C_5H_4CH{=}CBr_2)]$, **2a**, and alkyne $[Co(\eta^4\text{-}C_4Ph_4)(\eta^5\text{-}C_5H_4C\equiv CH)]$, **3a**. Both **4a** and **4b** undergo the normal aldehyde reactions with malononitrile and 2,4-dinitrophenylhydrazines to give their respective condensation products $[Co(\eta^4\text{-}C_4Ph_4)\{\eta^5\text{-}C_5H_4C\equiv C{-}CH{=}C(CN)_2\}]$, **5a**, and $[Fe(\eta^5\text{-}C_5H_5)\{\eta^5\text{-}C_5H_4C\equiv C{-}CH{=}C(CN)_2\}]$, **5b**; $[Co(\eta^4\text{-}C_4Ph_4)\{\eta^5\text{-}C_5H_4C\equiv C{-}CH{=}N{-}N(H)C_6H_3(NO_2)_2\text{-}2,4\}]$, **6a**, and $[Fe(\eta^5\text{-}C_5H_5)\{\eta^5\text{-}C_5H_4C\equiv C{-}CH{=}N{-}N(H)C_6H_3(NO_2)_2\text{-}2,4\}]$, **6b**, as separable mixtures of *syn*- and *anti*-isomers; and the *anti*-isomers of $[Co(\eta^4\text{-}C_4Ph_4)\{\eta^5\text{-}C_5H_4C\equiv C{-}CH{=}N{-}N(Me)C_6H_3(NO_2)_2\text{-}2,4\}]$, **7a**, and $[Fe(\eta^5\text{-}C_5H_5)\{\eta^5\text{-}C_5H_4C\equiv C{-}CH{=}N{-}N(Me)C_6H_3(NO_2)_2\text{-}2,4\}]$, **7b**. With $[Fe_2(\eta\text{-}C_5H_5)_2(CO)_2(\mu\text{-}CO)(\mu\text{-}CMe)][BF_4]$ **4a** and **4b** form blue-green $[Fe_2(\eta\text{-}C_5H_5)_2(CO)_2(\mu\text{-}CO)(\mu\text{-}C{-}CH{=}CH{-}C\equiv C{-}C_5H_4\text{-}\eta^5)Co(\eta^4\text{-}C_4Ph_4)][BF_4]$, [**8a**]$[BF_4]$, and black $[Fe_2(\eta\text{-}C_5H_5)_2(CO)_2(\mu\text{-}CO)(\mu\text{-}C{-}CH{=}CH{-}C\equiv C{-}C_5H_4\text{-}\eta^5)Fe(\eta^5\text{-}C_5H_5)][BF_4]$, [**8b**]$[BF_4]$ salts. **4a** and **4b** also react with the Wittig reagent $[Fe(\eta^5\text{-}C_5H_5)(\eta^5\text{-}C_5H_4{-}CH_2PPh_3)][I]/{}^{n}BuLi$ to give mixtures of *Z* and *E*-$[Co(\eta^4\text{-}C_4Ph_4)(\eta^5\text{-}C_5H_4{-}C\equiv C{-}CH{=}CH{-}C_5H_4\text{-}\eta^5)Fe(\eta^5\text{-}C_5H_5)]$, **9a**, and $[Fe(\eta^5\text{-}C_5H_5)(\eta^5\text{-}C_5H_4{-}C\equiv C{-}CH{=}CH{-}C_5H_4\text{-}\eta^5)Fe(\eta^5\text{-}C_5H_5)]$, **9b**, which are separable for **9b** but not **9a**. The Wittig reagent obtained from $[Co(\eta^4\text{-}C_4Ph_4)(\eta^5\text{-}C_5H_4{-}CH_2PPh_3)][Cl]/{}^{n}BuLi$ failed to react with **4a** or **4b**, but the reaction of **4a** with $[ClCH_2PPh_3][Cl]/{}^{t}BuOK$ gives very low yields of one expected product, *E*-$[Co(\eta^4\text{-}C_4Ph_4)(\eta^5\text{-}C_5H_4{-}C\equiv C{-}CH{=}CH{-}C_5H_4\text{-}\eta^5)Co(\eta^4\text{-}C_4Ph_4)]$, *E*-**10a**, together with a number of other unidentified compounds. The IR, ^1H NMR and ^{13}C NMR, and UV/Vis spectra of **4**–**9** are reported, assigned and discussed. They confirm that **4**–**9** are Donor–π–Acceptor complexes in which $Co(\eta^4\text{-}C_4Ph_4)(\eta^5\text{-}C_5H_4{-})$ is a weaker donor than $Fe(\eta^5\text{-}C_5H_5)(\eta^5\text{-}C_5H_4{-})$, the acceptor strength increases for Acceptor $= CH{=}CHFc < CH{=}N{-}N(R)C_6H_3(NO_2)_2\text{-}2,4 < CHO < CHC(CN)_2 < ({-}CH{=}CH{-}C_{\mu}^{+})(\mu\text{-}CO)(CO)_2Fe_2(\eta^5\text{-}C_5H_5)_2$, and that an ethyne linker, $\pi = C\equiv C$, is less effective than an ethene linker, $\pi = CH{=}CH$, in promoting electronic communication between the Donor and Acceptor. The molecular structures of **2a**, **3a**, **4a**, **4b**, **5b**, *syn*-**6a**, *syn*-**6b** (two crystal forms) and *anti*-**7b** have been determined by X-ray diffraction. They have normal molecular dimensions, and the $C_5H_4{-}C\equiv C{-}CH{=}Y$ moiety does not deviate greatly from planarity with angles between the C_5H_4 and $\equiv C{-}C(H){=}Y$ planes of 4.2–19.6°. This contrasts with the structures of $Fc{-}C\equiv C{-}R$ (R = aryl) complexes where the C_5H_4 and aryl planes are orthogonal or close to it. The electrochemistry of **3a**/**3b**, **4a**/**4b**, **5a**/**5b**, *syn*-**6a**/**6b**, *anti*-**7a**/**7b**, *E*/*Z*-**9a**, *Z*-**9b**, *E*-**9b** and $[Co(\eta^4\text{-}C_4Ph_4)(\eta^5\text{-}C_5H_4{-}C\equiv C{-}C_6H_5)]$ has been studied. The $Co(\eta^4\text{-}C_4Ph_4)(\eta^5\text{-}C_5H_4{-})$ complexes undergo reversible 1e oxidations at higher E° than their $Fe(\eta^5\text{-}C_5H_5)(\eta^5\text{-}C_5H_4{-})$ counterparts with E° increasing as the electron-withdrawing ability of the acceptor group increases. Furthermore, like their ferrocenyl counterparts, the alkyne derivatives $[Co(\eta^4\text{-}C_4Ph_4)(\eta^5\text{-}C_5H_4{-}C\equiv C{-}X)]$ are oxidised

---

* Corresponding author. Tel.: +64 3 479 4897; fax: +64 3 479 7906.
E-mail address: mcadamj@alkali.otago.ac.nz (C. John McAdam).

0022-328X/$ – see front matter
doi:10.1016/j.jorganchem.2011.12.012

at a more positive E° than the alkene complexes [Co(η^4-C_4Ph_4)(η^5-C_5H_4–CH=CH–X)]. The UV/Visible spectrum of the oxidized species [Co(η^4-C_4Ph_4)(η^5-C_5H_4–C≡C–C_6H_5)]$^+$ shows an absorption band at 960 nm due to a $C_6H_5 \rightarrow$ Co(η^4-C_4Ph_4)(η^5-C_5H_4–) charge transfer transition; its equivalent in the spectrum of [Fe(η^5-C_5H_5)(η^5-C_5H_4–C≡C–C_6H_5)]$^+$ is found at 797 nm. This implies that {Co(η^4-C_4Ph_4)(η^5-C_5H_4–)}$^+$ is a stronger acceptor than {Fe(η^5-C_5H_5)(η^5-C_5H_4–)}$^+$.

1. Introduction

A rich vein of chemistry has been the study of compounds which contain the structural motif EG–conjugated–EG′ where two end-groups EG– and EG′– are linked by an unsaturated conjugated spacer which allows electronic communication between them. The two end-groups can be the same or different. In the case of the latter one may act as an electron D(onor) and the other as an electron A(cceptor) in D–π–A systems. The conjugated linker may be based on an odd or even number of carbon atoms incorporating CR, ene, yne, aromatic and/or heteroaromatic systems with the proviso that each C atom in the linking chain is sp^2 or sp hybridised [1–3]. Surprisingly, among the less common are linkers which contain both ene and yne components i.e. EG–C≡C–CH=CH–EG′ systems [4–8], and here we describe some compounds containing them.

In a number of papers we have described EG-conjugated-EG′ compounds in which at least one of the end-groups is an organometallic moiety such as Fe(η^5-C_5H_5)(η^5-C_5H_4–) {= Fc–} [9,10], Co(η^4-C_4Ph_4)(η^5-C_5H_4–) {= Cb^φ–} [11–13], Ni(η^5-C_5H_5)(PPh_3)– [14] and Fe_2(η-C_5H_5)$_2$(CO)$_2$(μ-CO)(μ-C–)$^{0,+}$ groups [15]. In the first two the conjugated system of the linker interacts with the metal atom via the η^5-cyclopentadienyl ligand but in the last two it is bonded directly to the metal atom(s). Herein we describe the preparation of [Cb^φ–C≡C–CHO] from [Cb^φ–CHO] and its conversion to various [Cb^φ–C≡C–CH=Y] derivatives where CH=Y=CH=C(CN)$_2$, CH=N–N(H)C_6H_3(NO$_2$)$_2$-2,4, CH=N–N(Me)C_6H_3(NO$_2$)$_2$-2,4, Fe_2(η-C_5H_5)$_2$(CO)$_2$(μ-CO)(μ-C–CH=CH–)$^+$, CH=CHCb^φ and CH=CHFc. The corresponding [Fc–C≡C–CH=Y] complexes have also been prepared, and the spectra, structures and electrochemistries of the two series are compared, and their bonding discussed.

This work extends and complements the existing literature on [Co(η^4-C_4Ph_4)(η^5-C_5H_4-C≡C–X)] complexes [16–19]. There are a vast number of derivatives where a ferrocenyl group is conjugated through a η^5-C_5H_4–C(sp^2) or η^5-C_5H_4–C(sp) bond to (poly)ene, (poly)yne or related systems. A few recent examples are given [20], many others can be found in references [2, 6–10, 13–15], others will be referred to in the course of this paper.

2. Experimental

Unless otherwise stated, all reactions were carried out at room temperature under an atmosphere of nitrogen in dried and deoxygenated solvents.

Previously reported procedures or closely related ones were used to prepare [Co(η^4-C_4Ph_4)(η^5-C_5H_4CHO)] **1a** [16], [Fe(η^5-C_5H_5)(η^5-C_5H_4CHO)] **1b** [21], [Fe(η^5-C_5H_5)(η^5-$C_5H_4CH_2PPh_3$)]I [22], [$ClCH_2PPh_3$]Cl [23], 1-methyl-1-(2,4-dinitro-phenyl)hydrazine [24], and [Fe_2(η^5-C_5H_5)$_2$(CO)$_2$(μ-CO)(μ-CCH_3)][BF_4] [25]. Other reagents were purchased from commercial sources unless otherwise stated. Column chromatography was performed on alumina (activity II or III) or silica (Merck 7734).

Infrared spectra were recorded on a Perkin Elmer Paragon 1000 FTIR spectrometer (resolution = 4 cm^{-1}), UV/visible spectra on a UNICAM UV2 spectrometer and NMR spectra on Varian Inova 300 or 500 MHz spectrometers. Elemental analyses were carried out in the Microanalytical Laboratory, University College Dublin, however most results were outside the generally accepted limits for conformity. There is crystallographic evidence for inclusion of solvent in two compounds and NMR suggests this is a likely compounding factor in other samples.

Cyclic voltammetric and differential pulse experiments were carried out at 20 °C in CH_2Cl_2 solutions degassed with nitrogen. A three-electrode cell was used with Cypress Systems 1 mm diameter Pt working, Ag/AgCl reference and platinum wire auxiliary electrodes. Solutions were $\sim 10^{-3}$ M in electroactive material and contained 0.1 M [Bu_4N][PF_6] as the supporting electrolyte. Voltammograms were recorded using a Powerlab/4sp computer-controlled potentiostat. All potentials are referenced to the reversible formal potential (taken as $E^\circ = 0.00$ V) for the decamethylferrocene [Fe(η^5-C_5Me_5)$_2$]$^{+/0}$ process [26] where E° was calculated from the average of the oxidation and reduction peak potentials under conditions of cyclic voltammetry. Under the same conditions, E° calculated for [Fe(η^5-C_5H_5)$_2$]$^{+/0}$ was 0.55 V.

2.1. *Preparation of [Co(η^4-C_4Ph_4)(η^5-C_5H_4–CH=CBr_2)],* ***2a****, and [Fe(η^5-C_5H_5)(η^5-C_5H_4–CH=CBr_2)],* ***2b***

A solution of PPh_3 (0.65 g, 2.50 mmol) and CBr_4 (0.42 g, 1.25 mmol) in anhydrous CH_2Cl_2 (50 mL) at 0 °C was stirred for 10 min until it turned dark orange. [Co(η^4-C_4Ph_4)(η^5-C_5H_4–CHO)], **1a** (0.51 g, 1.0 mmol) was added and the reaction mixture stirred at room temperature. After 2 h, pentane (250 mL) was added to it, and the precipitate filtered off. This was dissolved in CH_2Cl_2 and precipitated again with pentane. The procedure was repeated until the filtrate was almost colourless. The filtrates were combined, concentrated, and chromatographed (silica-pentane) to afford [Co(η^4-C_4Ph_4)(η^5-C_5H_4–CH=CBr_2)], **2a**, as a brown crystalline solid (Yield 0.49 g, 74%).

This procedure was used to convert [Fe(η^5-C_5H_5)(η^5-C_5H_4–CHO)], **1b**, to [Fe(η^5-C_5H_5)(η^5-C_5H_4–CH=CBr_2)], **2b**, an orange crystalline solid (Yield 0.33 g, 90%).

2.1.1. *[Co(η^4-C_4Ph_4)(η^5-C_5H_4–CH=CBr_2)],* ***2a***

^{1}H NMR ($CDCl_3$): δ 7.20–7.44 (20H, m, C_6H_5), 6.42 (1H, s, CH=CBr_2), 5.01 (2H, t, C_5H_4Co), 4.72 (2H, t, C_5H_4Co). ^{13}C NMR ($CDCl_3$): δ 137.7 (CH=CBr_2), 135.5, 129.2, 128.3, 125.4 (C_6H_5), 92.1, 84.8, 83.1 (η^5-C_5H_4Co), 85.1 (CH=CBr_2), 77.0 (C_4Ph_4). UV–Vis, λ_{max}/nm ($\varepsilon \times 10^{-3}$/dm^{3}mol^{-1}cm^{-1}) (CH_2Cl_2): 260 (48), 300 (33), 391 (10).

2.2. *Preparation of [Co(η^4-C_4Ph_4)(η^5-C_5H_4–C≡CH)],* ***3a****, and [Fe(η^5-C_5H_5)(η^5-C_5H_4–C≡CH)],* ***3b***

A 1.6 *M* solution of ^{n}BuLi (1.40 mL, 2.20 mmol) in hexane was added drop-wise to a stirred solution of **2a**, (0.66 g, 1.0 mmol) in anhydrous Et_2O/THF (2/1; 60 mL) at −78 °C. After 1 h, the mixture was allowed to warm to room temperature. After a further 2 h, the mixture was added to water (50 mL), the organic layer was extracted with CH_2Cl_2 (3 x 20 mL), and the combined extracts dried over $MgSO_4$. Removal of the solvent gave the crude product which was chromatographed on silica (pentane/CH_2Cl_2; 1/1) to afford [Co(η^4-C_4Ph_4)(η^5-C_5H_4–C≡CH)], **3a**, as a brown crystalline solid (Yield 0.42 g, 83%).

2b was converted to dark orange crystalline $[Fe(\eta^5-C_5H_5)(\eta^5-C_5H_4-C\equiv CH)]$, **3b**, using the same procedure (Yield 0.19 g, 90%). Characterisation for **3a** and **3b** is as previously reported (see also Supplementary material).

2.3. Preparation of $[Co(\eta^4-C_4Ph_4)(\eta^5-C_5H_4-C\equiv C-CHO)]$, **4a**, and $[Fe(\eta^5-C_5H_5)(\eta^5-C_5H_4-C\equiv C-CHO)]$, **4b**

A 1.6 M solution of ^nBuLi (1.60 mL, 2.50 mmol) in hexane was added to one of **3a**, (1.21 g, 2.40 mmol) in tetrahydrofuran, THF, (20 mL) at −78 °C followed, after 30 min, by an excess of DMF (0.50 mL, 6.50 mmol). After a further hour at −78 °C, the mixture was brought to room temperature and poured over ice-water (25 mL) containing concentrated hydrochloric acid (2 mL). The violet mixture was neutralised with $NaHCO_3$ solution to give a red solution which was extracted with Et_2O. The extracts were dried over $MgSO_4$, filtered and chromatographed on silica (pentane/CH_2Cl_2; 1/1). Removal of the solvent gave $[Co(\eta^4-C_4Ph_4)(\eta^5-C_5H_4-C\equiv C-CHO)]$, **4a** as an orange/brown crystalline solid (Yield 0.79 g, 62%).

3b was converted to red crystalline $[Fe(\eta^5-C_5H_5)(\eta^5-C_5H_4-C\equiv C-CHO)]$, **4b**, using the same procedure (Yield 0.52 g, 91%).

2.3.1. $[Co(\eta^4-C_4Ph_4)(\eta^5-C_5H_4-C\equiv C-CHO)]$, **4a**

IR ν/cm^{-1}: $\nu(C\equiv C)$ 2181, $\nu(CHO)$ 1649 (CH_2Cl_2); $\nu(C\equiv C)$ 2178, $\nu(CHO)$ 1646 (KBr). ^1H NMR ($CDCl_3$): δ 8.83 (1H, s, CHO), 7.11–7.53 (20H, m, C_6H_5), 4.95 (2H, t, C_5H_4Co), 4.82 (2H, t, C_5H_4Co). ^{13}C NMR ($CDCl_3$): δ 176.6 (CHO), 134.9, 129.1, 128.4, 127.1 (C_6H_5), 95.5 ($C\equiv CCHO$), 88.6 ($C\equiv CCHO$), 88.0, 86.9, 74.1 (C_5H_4Co), 77.5 (C_4Ph_4). UV–Vis, λ_{max}/nm ($\varepsilon \times 10^{-3}/dm^3\ mol^{-1}\ cm^{-1}$) ($CH_2Cl_2$): 272 (38), 335 (sh, 20), 392 (sh, 4.3).

2.4. Preparation of $[Co(\eta^4-C_4Ph_4)(\eta^5-C_5H_4-C\equiv C-CH=C(CN)_2\}]$, **5a**, and $[Fe(\eta^5-C_5H_5)\{\eta^5-C_5H_4-C\equiv C-CH=C(CN)_2\}]$, **5b**

To solutions of the acetylenic aldehydes, **4a** or **4b** (1.0 mmol), in anhydrous CH_2Cl_2 (50 mL) was added a ca. equimolar amount of malononitrile (0.075 g, 1.10 mmol) and 3 drops of Et_3N. The reaction mixtures immediately changed colour and were stirred for 2 h in the absence of light. They were concentrated to dryness and the residues chromatographed on silica (Et_2O/pentane; 1/1) to afford dark red crystals of $[Co(\eta^4-C_4Ph_4)(\eta^5-C_5H_4-C\equiv C-CH=C(CN)_2\}]$, **5a**, (Yield 0.47 g, 80%) or violet crystals of $[Fe(\eta^5-C_5H_5)\{\eta^5-C_5H_4-C\equiv C-CH=C(CN)_2\}]$, **5b**, (Yield 0.27 g, 95%).

2.4.1. $[Co(\eta^4-C_4Ph_4)\{\eta^5-C_5H_4-C\equiv C-CH=C(CN)_2\}]$, **5a**

IR ν/cm^{-1}: $\nu(C\equiv N)$ 2224, $\nu(C\equiv C)$ 2176 (CH_2Cl_2); $\nu(C\equiv N)$ 2224, $\nu(C\equiv C)$ 2172 (KBr). ^1H NMR ($CDCl_3$): δ 7.20–7.48 (20H, m, C_6H_5), 6.51 {1H, s, $CH=C(CN)_2$}, 4.97 (2H, t, C_5H_4Co), 4.91 (2H, t, C_5H_4Co). ^{13}C NMR ($CDCl_3$): δ 142.0 {$CH=C(CN)_2$}, 134.0, 129.0, 128.0, 127.0 (C_6H_5), 116.5 {$CH=C(CN)_2$}, 113.5, 113.0 (CN) 88.0, 87.8, 74.2 (C_5H_4Co), 88.2 {$C\equiv CCHC(CN)_2$}, 85.8 {$C\equiv CCHC(CN)_2$}, 77.8 (C_4Ph_4). UV–Vis, λ_{max}/nm ($\varepsilon \times 10^{-3}/dm^3mol^{-1}cm^{-1}$) ($CH_2Cl_2$): 276 (30), 343 (12), 465 (6.7).

2.4.2. $[Fe(\eta^5-C_5H_5)\{\eta^5-C_5H_4-C\equiv C-CH=C(CN)_2\}]$, **5b**

IR ν/cm^{-1}: $\nu(C\equiv N)$ 2230, $\nu(C\equiv C)$ 2175 (CH_2Cl_2); $\nu(C\equiv N)$ 2230, $\nu(C\equiv C)$ 2175 (KBr). ^1H NMR ($CDCl_3$): δ 7.03 {1H, s, $CH=C(CN)_2$}, 4.66 (2H, t, C_5H_4Fe), 4.56 (2H, t, C_5H_4Fe), 4.30 (5H, s, C_5H_5Fe). ^{13}C NMR ($CDCl_3$): δ 141.4 {$CH=C(CN)_2$}, 120.9 {$CH=C(CN)_2$}, 113.6, 112.4 (CN), 90.3 {$C\equiv CCHC(CN)_2$}, 84.7 {$C\equiv CCHC(CN)_2$}, 73.7, 72.5, 60.4 (C_5H_4Fe), 71.2 (C_5H_5Fe). UV–Vis, λ_{max}/nm ($\varepsilon \times 10^{-3}/dm^3mol^{-1}cm^{-1}$) ($CH_2Cl_2$): 281 (17), 362 (35), 560 (10).

2.5. The reactions of $[Co(\eta^4-C_4Ph_4)(\eta^5-C_5H_4-C\equiv C-CHO)]$, **4a**, and $[Fe(\eta^5-C_5H_5)(\eta^5-C_5H_4-C\equiv C-CHO)]$, **4b**, with 2,4-dinitrophenylhydrazine and 1-methyl-1-(2,4-dinitrophenyl)hydrazine

To a solution of the acetylenic aldehydes, **4a** or **4b** (1.0 mmol) in anhydrous CH_2Cl_2 (50 mL) was added an equimolar amount of 2,4-dinitro-phenylhydrazine (0.28 g, 1.0 mmol) plus 4 drops of glacial acetic acid. The reaction mixtures were stirred at room temperature for 3 h, after which time the solvent was removed under reduced pressure. The residue was chromatographed on silica (pentane/CH_2Cl_2; 1/1) to afford similar amounts of *syn-* and *anti-* isomers of the hydrazones $[Co(\eta^4-C_4Ph_4)\{\eta^5-C_5H_4-C\equiv CCH=N-N(H)C_6H_3(NO_2)_2-2,4\}]$, **6a**, or $[Fe(\eta^5-C_5H_5)\{\eta^5-C_5H_4-C\equiv CCH=N-N(H)C_6H_3(NO_2)_2-2,4\}]$, **6b**, as dark red crystalline solids in 30–45% yields.

Under the same conditions **4a** and **4b** react with 1-methyl-1-(2,4-dinitrophenyl)hydrazine to give $[Co(\eta^4-C_4Ph_4)\{\eta^5-C_5H_4-C\equiv CCH=N-N(Me)C_6H_3(NO_2)_2-2,4\}]$, **7a**, or $[Fe(\eta^5-C_5H_5)\{\eta^5-C_5H_4-C\equiv C-CH=N-N(Me)C_6H_3(NO_2)_2-2,4\}]$, **7b**, as orange red crystalline solids in yields of 55 and 80% respectively.

2.5.1. Syn-$[Co(\eta^4-C_4Ph_4)\{\eta^5-C_5H_4-C\equiv C-CH=N-N(H)C_6H_3(NO_2)_2-2,4\}]$, syn-**6a**

IR ν/cm^{-1}: $\nu(C\equiv C)$ 2184 (CH_2Cl_2); $\nu(C\equiv C)$ 2183 (KBr). ^1H NMR ($CDCl_3$): δ 11.45 (1H, s, CH=NNH), 9.15 {1H, d, J = 2 Hz, $C_6H_3(NO_2)_2$}, 8.36 {1H, dd, J = 2, 10 Hz, $C_6H_3(NO_2)_2$}, 7.92, J = 10 Hz {1H, d, $C_6H_3(NO_2)_2$}, 7.15–7.44 (20H, m, C_6H_5), 6.70 (1H, s, CH=NNH), 5.12 (2H, t, C_5H_4Co), 4.82 (2H, t, C_5H_4Co). ^{13}C NMR ($CDCl_3$): δ 144.1, 138.6, 130.0, 129.5, 123.4, 116.8 {$C_6H_3(NO_2)_2$}, 134.9, 128.8, 128.1, 126.6 (C_6H_5), 126.5 (CH=N), 103.9 ($C\equiv CCH=N$), 79.5 ($C\equiv CCH=N$), 87.3, 86.1, 75.4 (C_5H_4Co), 77.1 (C_4Ph_4). UV–Vis, λ_{max}/nm ($\varepsilon \times 10^{-3}/dm^3mol^{-1}cm^{-1}$) ($CH_2Cl_2$): 268 (63), 334 (31), 374 (32), 412 (27).

2.5.2. Anti-$[Co(\eta^4-C_4Ph_4)\{\eta^5-C_5H_4-C\equiv C-CH=N-N(H)C_6H_3(NO_2)_2-2,4\}]$, anti-**6a**

IR ν/cm^{-1}: $\nu(C\equiv C)$ 2205 (CH_2Cl_2); $\nu(C\equiv C)$ 2197 (KBr). ^1H NMR ($CDCl_3$): δ 11.30 (1H, s, CH=NNH), 9.12 {1H, d, J = 2 Hz, $C_6H_3(NO_2)_2$}, 8.30 {1H, dd, J = 2, 10 Hz, $C_6H_3(NO_2)_2$}, 7.90 {1H, d, J = 10 Hz, $C_6H_3(NO_2)_2$}, 7.12–7.39 (20H, m, C_6H_5), 7.02 (1H, s, CH=NNH), 4.93 (2H, t, C_5H_4Co), 4.72 (2H, t, C_5H_4Co). ^{13}C NMR ($CDCl_3$): δ 144.2, 135.1, 131.8, 130.2, 129.9, 117.1 {$C_6H_3(NO_2)_2$}, 135.1, 128.9, 128.1, 126.7 (C_6H_5), 123.9 (CH=N), 95.2 ($C\equiv CCH=N$), 82.6 ($C\equiv CCH=N$), 86.6, 85.9, 77.5 (C_5H_4Co), 76.8 (C_4Ph_4). UV–Vis, λ_{max}/nm ($\varepsilon \times 10^{-3}/dm^3mol^{-1}cm^{-1}$) ($CH_2Cl_2$): 329 (12), 464 (9).

2.5.3. Syn-$[Fe(\eta^5-C_5H_5)\{\eta^5-C_5H_4-C\equiv C-CH=N-N(H)C_6H_3(NO_2)_2-2,4\}]$, syn-**6b**

IR ν/cm^{-1}: $\nu(C\equiv C)$ 2186 (CH_2Cl_2); ν $(C\equiv C)$ 2178 (KBr). ^1H NMR ($CDCl_3$): δ 12.12 (1H, s, CH=N–NH), 9.19 {1H, d, J = 2 Hz, $C_6H_3(NO_2)_2$}, 8.38 {1H, dd, J = 2, 10 Hz,$C_6H_3(NO_2)_2$}, 8.00 {1H, d, J = 10 Hz, $C_6H_3(NO_2)_2$}, 6.93 (1H, s, CH=N–NH), 4.74 (2H, t, C_5H_4Fe), 4.43 (2H, t, C_5H_4Fe), 4.28 (5H, s, C_5H_5Fe). ^{13}C NMR ($CDCl_3$): δ 144.2, 138.7, 130.1, 129.8, 123.5, 117.1 {$C_6H_3(NO_2)_2$}, 126.9 (CH=N), 107.8 ($C\equiv CCH=N$), 76.8 ($C\equiv CCH=N$), 72.7, 70.8, 60.9 (C_5H_4Fe), 70.7 (C_5H_5Fe). UV–Vis, λ_{max}/nm ($\varepsilon \times 10^{-3}/dm^3mol^{-1}cm^{-1}$) ($CH_2Cl_2$): 266 (37), 314 (sh), 374 (27), 444 (sh).

2.5.4. Anti-$[Fe(\eta^5-C_5H_5)\{\eta^5-C_5H_4-C\equiv C-CH=N-N(H)C_6H_3(NO_2)_2-2,4\}]$, anti-**6b**

IR ν/cm^{-1}: $\nu(C\equiv C)$ 2203 (CH_2Cl_2); $\nu(C\equiv C)$ 2191 (KBr). ^1H NMR ($CDCl_3$): δ 11.45 (1H, s, CH=NNH), 9.14 {1H, d, J = 2 Hz, $C_6H_3(NO_2)_2$}, 8.36 {1H, dd, J = 2, 10 Hz, $C_6H_3(NO_2)_2$}, 8.04 {1H, d, J = 10 Hz, $C_6H_3(NO_2)_2$}, 7.47 (1H, s, CH=NNH), 4.58 (2H, t, C_5H_4Fe), 4.36 (2H, t, C_5H_4Fe), 4.28 (5H, s, C_5H_5Fe). ^{13}C NMR ($CDCl_3$): δ 144.4, 138.2, 131.3, 130.1, 123.2, 117.2 {$C_6H_3(NO_2)_2$}, 123.3 (CH=N), 81.5 ($C\equiv CCH=N$), 70.7 ($C\equiv CCH=N$), 72.2, 70.6, 62.1 (C_5H_4Fe), 70.3 (C_5H_5Fe). UV–Vis, λ_{max}/nm ($\varepsilon \times 10^{-3}$/dm^{3}mol^{-1}cm^{-1}) (CH_2Cl_2): 267 (43), 314 (6.8), 375 (30), 494 sh (3.1).

2.5.5. Anti-$[Co(\eta^4-C_4Ph_4)\{\eta^5-C_5H_4-C\equiv C-CH=N-N(Me)C_6H_3(NO_2)_2-2,4\}]$, anti-*7a*

IR ν/cm^{-1}: $\nu(C\equiv C)$ 2207 (CH_2Cl_2); $\nu(C\equiv C)$ 2188 (KBr). ^1H NMR ($CDCl_3$): δ 8.68 {1H, d, $J = 2$ Hz, $C_6H_3(NO_2)_2$}, 8.30 {1H, dd, $J = 2$, 10 Hz $C_6H_3(NO_2)_2$}, 7.66 {1H, d, $J = 10$ Hz, $C_6H_3(NO_2)_2$}, 7.22–7.47 (20H, m, C_6H_5), 6.48 (1H, s, $CH=N$), 4.84 (2H, t, C_5H_4Co), 4.72 (2H, t, C_5H_4Co), 3.26 (3H, s, NCH_3). ^{13}C NMR ($CDCl_3$): δ 145.8, 142.7, 127.2, 122.5, 121.5, 118.0 {$C_6H_3(NO_2)_2$}, 135.2, 128.9, 128.0, 126.4 (C_6H_5), 123.4 ($CH=NN$), 91.4 ($C\equiv CCH=N$), 86.4, 85.1, 76.9 (C_5H_4Co), 82.7 ($C\equiv CCH=N$), 76.4 (C_4Ph_4), 36.9 (NCH_3). UV–Vis, λ_{max}/nm ($\varepsilon \times 10^{-3}$/dm^{3}mol^{-1}cm^{-1}) (CH_2Cl_2): 272 (42), 335 (24), 413 (22).

2.5.6. Anti-$[Fe(\eta^5-C_5H_5)\{\eta^5-C_5H_4-C\equiv C-CH=N-N(Me)C_6H_3(NO_2)_2-2,4\}]$, anti-*7b*

IR ν/cm^{-1}: (CH_2Cl_2) $\nu(C\equiv C)$ 2205 (CH_2Cl_2); $\nu(C\equiv C)$ 2200, $\nu(C=N)$ 1597, $\nu(C=C)$ 1599, 1500, $\nu(NO)$ 1541, 1316 (KBr). ^1H NMR ($CDCl_3$): δ 8.65 (1H, d, $J = 2$ Hz, $C_6H_3(NO_2)_2$), 8.32 {1H, dd, $J = 2$, 10 Hz, $C_6H_3(NO_2)_2$}, 7.63 {1H, d, $J = 10$ Hz $C_6H_3(NO_2)_2$}, 6.99 (1H, s, $CH=NN$), 4.57 (2H, t, C_5H_4Fe), 4.37 (2H, t, C_5H_4Fe), 4.30 (5H, s, C_5H_5Fe), 3.35 (3H, s, NCH_3). ^{13}C NMR ($CDCl_3$): δ 145.8, 140.8, 139.3, 127.3, 122.5, 121.3 {$C_6H_3(NO_2)_2$}, 123.2 ($CH=N$), 94.7 ($C\equiv CCH=N$), 81.3 ($C\equiv CH=N$), 71.8, 69.8, 63.3 (C_5H_4Fe), 70.2 (C_5H_5Fe), 36.5 (NCH_3). UV–Vis, λ_{max}/nm ($\varepsilon \times 10^{-3}$/dm^{3}mol^{-1}cm^{-1}) (CH_2Cl_2): 308 (18), 395 (28), 464 (sh).

2.6. The reactions of $[Co(\eta^4-C_4Ph_4)(\eta^5-C_5H_4-C\equiv C-CHO)]$, **4a**, and $[Fe(\eta^5-C_5H_5)(\eta^5-C_5H_4-C\equiv C-CHO)]$, **4b**, with $[Fe_2(\eta-C_5H_5)_2(CO)_2(\mu-CO)(\mu-CCH_3)][BF_4]$

$[Fe_2(\eta^5-C_5H_5)_2(CO)_2(\mu-CO)(\mu-CCH_3)][BF_4]$ (0.36 g, 0.83 mmol) was dissolved in CH_2Cl_2 (70 mL) and the solution brought to reflux. The acetylenic aldehydes **4a** or **4b** (1.0 mmol, 1.2 equiv.) were then added and the solutions allowed to stir under reflux in the dark for 24 h. The volume of the filtered solutions were then reduced to approximately 20 mL, layered with Et_2O, and allowed to stand at −5 °C. The products, green-black $[Fe_2(\eta-C_5H_5)_2(CO)_2(\mu-CO)(\mu-C-CH=CH-C\equiv C-Cb^{\varphi})][BF_4]$, [**8a**][BF$_4$], {$Cb^{\varphi} = Co(\eta^4-C_4Ph_4)(\eta^5-C_5H_4-)$} or black $[Fe_2(\eta-C_5H_5)_2(CO)_2(\mu-CO)(\mu-C-CH=CH-C\equiv C-Fc)][BF_4]$, [**8b**][BF$_4$], {$Fc = Fe(\eta^5-C_5H_5)(\eta^5-C_5H_4-)$} precipitated as microcrystalline powders in yields of 80% and 90% respectively.

2.6.1. $[Fe_2(\eta^5-C_5H_5)_2(CO)_2(\mu-CO)(\mu-C-CH=CH-C\equiv C-C_5H_4-\eta^5)Co(\eta^4-C_4Ph_4)][BF_4]$, [*8a*][BF$_4$]

IR ν/cm^{-1}: $\nu(C\equiv C)$ 2148, $\nu(CO)$ 2033, 2004, $\nu(\mu-CO)$ 1848 (CH_2Cl_2); $\nu(C\equiv C)$ 2154, $\nu(CO)$ 2024, 1995, $\nu(\mu-CO)$ 1845 (KBr). ^1H NMR ($CDCl_3$): δ 8.92 (1H, d, $J = 14$ Hz, $C_{\mu}-CH=CH$), 7.12–7.47 (20H, m, C_6H_5), 6.58 (1H, d, $J = 14$ Hz, $C_{\mu}-CH=CH$), 5.37 {10H, s, $(C_5H_5)_2Fe_2$}, 5.08 (2H, t, C_5H_4Co), 4.99 (2H, t, C_5H_4Co). ^{13}C NMR ($CDCl_3$): δ 435.8 (C_{μ}), 254.1 (μ-CO), 209.3 (t-CO), 159.9 ($C_{\mu}-CH=CH$), 134.6 ($C_{\mu}-CH=CH$), 135.7, 130.0, 129.5, 128.2 (C_6H_5), 118.7 ($C\equiv CCH=CH$), 94.0 ($C\equiv CCH=CH$), 91.5, 89.4, 88.8 (C_5H_4Co), 93.4 (C_5H_5Fe), 79.4 (C_4Ph_4). UV–Vis, λ_{max}/nm ($\varepsilon \times 10^{-3}$/dm^{3}mol^{-1}cm^{-1}) (CH_2Cl_2): 275 (50), 416 (20), 659 (19).

2.6.2. $[Fe_2(\eta^5-C_5H_5)_2(CO)_2(\mu-CO)(\mu-CCH=CH-C\equiv C-C_5H_4-\eta^5)Fe(\eta^5-C_5H_5)][BF_4]$. [*8b*][BF$_4$]

IR ν/cm^{-1}: $\nu(C\equiv C)$ 2147, $\nu(CO)$ 2033, 1996(sh), $\nu(\mu-CO)$ 1844 (CH_2Cl_2); $\nu(C\equiv C)$ 2149, $\nu(CO)$ 2012, 1998, $\nu(\mu-CO)$ 1831(KBr). ^1H NMR ($CDCl_3$): δ 9.35 (1H, d, $J = 14$ Hz, $C_{\mu}-CH=CH$), 6.96 (1H, d, $J = 14$ Hz, $C_{\mu}-CH=CH$), 5.36 {10H, s, $(C_5H_5)_2Fe_2$}, 4.78 (2H, t, C_5H_4Fe), 4.73 (2H, t, C_5H_4Fe), 4.44 (5H, s, C_5H_5Fe). UV–Vis, λ_{max}/nm ($\varepsilon \times 10^{-3}$/dm^{3}mol^{-1}cm^{-1}) (CH_2Cl_2): 329 (12), 464 (9), 644 (6.6), 722 (6.0).

2.7. The reactions of $[Co(\eta^4-C_4Ph_4)(\eta^5-C_5H_4C\equiv CCHO)]$, *4a*, and $[Fe(\eta^5-C_5H_5)(\eta^5-C_5H_4-C\equiv C-CHO)]$, *4b*, with $[Fe(\eta^5-C_5H_5)(\eta^5-C_5H_4-CH_2PPh_3)][I]/^nBuLi$

A hexane solution of ^nBuLi (1.6 *M*, 0.72 mL, 1.10 mmol) was added to an orange suspension of $[Fe(\eta^5-C_5H_5)(\eta^5-C_5H_4-CH_2PPh_3)][I]$ (0.58 g, 1.0 mmol) in anhydrous THF (30 mL) at −78 °C. After stirring at −78 °C for 1 h the acetylenic aldehydes, **4a** or **4b** (1.0 mmol) were added to the reaction mixtures which were then allowed to warm to room temperature, stirred for 2 h, and added to deionised water (10 mL). The organic phases were extracted with CH_2Cl_2, dried over $MgSO_4$ and concentrated to dryness. The crude products were chromatographed on silica (pentane/CH_2Cl_2; 2:1) to yield a *Z*/*E* mix of $[Co(\eta^4-C_4Ph_4)(\eta^5-C_5H_4-C\equiv C-CH=CH-Fc)]$, **9a**, (Yield 0.28 g, ~5:3 *Z*:*E* from NMR), and resolved *Z* and *E* isomers of $[Fe(\eta^5-C_5H_5)(\eta^5-C_5H_4-C\equiv C-CH=CH-Fc)]$, **9b**, (Yields 0.08 g, 20% each isomer).

2.7.1. E/Z-$[Co(\eta^4-C_4Ph_4)(\eta^5-C_5H_4-C\equiv C-CH=CH-C_5H_4-\eta^5)Fe(\eta^5-C_5H_5)]$, E/Z-*9a*

IR ν/cm^{-1}: $\nu(C\equiv C)$ 2194 (CH_2Cl_2); $\nu(C\equiv C)$ 2184 (KBr). UV–Vis, λ_{max}/nm ($\varepsilon \times 10^{-3}$/dm^{3}mol^{-1}cm^{-1}) (CH_2Cl_2) 260 (50), 290 (sh 40), 335 (29), 386 (sh 12), 464 (sh 6.4).

Z-**9a**. ^1H NMR ($CDCl_3$): δ 7.16–7.50 (20H, m, C_6H_5), 6.32 (1H, d, $J = 11$ Hz, $C\equiv CCH=CH$), 5.24 (1H, d, $J = 11$ Hz, $C\equiv CCH=CH$), 4.79 (2H, t, C_5H_4Co), 4.69 (2H, t, C_5H_4Co), 4.65 (2H, t, C_5H_4Fe), 4.23 (2H, t, C_5H_4Fe), 4.07 (5H, s, C_5H_5Fe). ^{13}C NMR ($CDCl_3$): δ 137.0 ($C\equiv CCH=CH$), 135.6, 128.9, 128.0, 126.4 (C_6H_5), 104.9 ($C\equiv CCH=CH$), 90.5 ($C\equiv CCH=CH$), 88.0. ($C\equiv CCH=CH$), 85.7, 84.5, 80.6 (C_5H_4Co), 81.4, 69.3, 69.3 (C_5H_4Fe), 76.1 (C_4Ph_4), 69.2 (C_5H_5Fe).

E-**9a**. ^1H NMR ($CDCl_3$): δ 7.16–7.50 (20H, m, C_6H_5), 6.40 (1H, d, $J = 16$ Hz, $C\equiv CCH=CH$), 5.58 (1H, d, $J = 16$ Hz, $C\equiv CCH=CH$), 4.76 (2H, t, C_5H_4Co), 4.63 (2H, t, C_5H_4Co), 4.37 (2H, t, C_5H_4Fe), 4.30 (2H, t, C_5H_4Fe), 4.14 (5H, s, C_5H_5Fe). ^{13}C NMR ($CDCl_3$): δ 139.1 ($C\equiv CCH=CH$), 135.7, 129.0, 128.0, 126.4 (C_6H_5), 105.4 ($C\equiv CCH=CH$), 87.8 ($C\equiv CCH=CH$), 85.5 ($C\equiv CCH=CH$), 85.5, 84.4, 80.0 (C_5H_4Co), 82.3, 69.5, 66.8 (C_5H_4Fe), 76.2 (C_4Ph_4), 69.6 (C_5H_5Fe).

2.7.2. Z-$[Fe(\eta^5-C_5H_5)(\eta^5-C_5H_4-C\equiv C-CH=CH-C_5H_5-\eta^5)Fe(\eta^5-C_5H_5)]$, Z-*9b*

IR ν/cm^{-1}: $\nu(C\equiv C)$ 2194 (CH_2Cl_2); $\nu(C\equiv C)$ 2187 (KBr). ^1H NMR ($CDCl_3$): δ 6.43 (1H, d, $J = 12$ Hz, $C\equiv CCH=CH$), 5.57 (1H, d, $J = 12$ Hz, $C\equiv CCH=CH$), 4.89 (2H, t, $C_5H_4Fe-C_{sp2}$), 4.52 (2H, t, $C_5H_4Fe-C_{sp}$), 4.35 (2H, t, $C_5H_4Fe-C_{sp2}$), 4.28 (5H, s, $C_5H_5Fe-C_{sp}$), 4.27 (2H, t, $C_5H_4Fe-C_{sp}$), 4.19 (5H, s, $C_5H_5Fe-C_{sp2}$). ^{13}C NMR ($CDCl_3$): δ 137.3 ($C\equiv CCH=CH$], 104.8 ($C\equiv CCH=CH$), 94.0 ($C\equiv CCH=CH$), 85.8 ($C\equiv CCH=CH$), 81.4 ($C_5H_4Fe-C_{sp}2$), 71.1 ($C_5H_4Fe-C_{sp}$), 70.0 ($C_5H_5Fe-C_{sp}$), 69.6 ($C_5H_5Fe-C_{sp2}$), 69.4 ($C_5H_4Fe-C_{sp}2$), 69.3 ($C_5H_4Fe-C_{sp}2$), 68.9 ($C_5H_4Fe-C_{sp}$), 66.2 ($C_5H_4Fe-C_{sp}$). UV–Vis, λ_{max}/nm ($\varepsilon \times 10^{-3}$/dm^{3}mol^{-1}cm^{-1}) (CH_2Cl_2): 284 (14), 320 (14), 373 (sh), 458 (1.6).

2.7.3. E-$[Fe(\eta^5-C_5H_5)(\eta^5-C_5H_4-C\equiv C-CH=CH-C_5H_5-\eta^5)Fe(\eta^5-C_5H_5)]$, E-*9b*

IR ν/cm^{-1}: $\nu(C\equiv C)$ 2195 (CH_2Cl_2); $\nu(C\equiv C)$ 2196, 2164 (KBr). ^1H NMR ($CDCl_3$): δ 6.72 (1H, d, $J = 16$ Hz, $C\equiv C-CH=CH$), 5.81 (1H, d, $J = 16$ Hz, $C\equiv C-CH=CH$), 4.45 (2H, t, $C_5H_4Fe-C_{sp}$), 4.43 (2H, t, $C_5H_4Fe-C_{sp2}$), 4.34 (2H, t, $C_5H_4Fe-C_{sp2}$), 4.25 (5H, s, $C_5H_5Fe-C_{sp}$), 4.23 (2H, t, $C_5H_4Fe-C_{sp}$), 4.21 (5H, s, $C_5H_5Fe-C_{sp2}$). ^{13}C NMR ($CDCl_3$): δ 139.1 ($C\equiv CCH=CH$], 105.4 ($C\equiv CCH=CH$), 89.0 ($C\equiv C-CH=CH$), 85.8 ($C\equiv C-CH=CH$), 83.1 ($C_5H_4Fe-C_{sp}2$), 71.2 ($C_5H_4Fe-C_{sp}$), 70.0 ($C_5H_5Fe-C_{sp}$), 69.8 ($C_5H_5Fe-C_{sp2}$), 69.8 ($C_5H_4Fe-C_{sp}2$), 68.8 (C_5H_4Fe-

C_{sp}), 67.0 (C_5H_4Fe-$C_{sp}2$), 66.2 (C_5H_4Fe-C_{sp}). UV–Vis, λ_{max}/nm ($\varepsilon \times 10^{-3}$/dm^{3}mol^{-1}cm^{-1}) (CH_2Cl_2):257 (20), 320 (24), 459 (21).

2.8. The reaction of [Co(η^4-C_4Ph_4)(η^5-C_5H_4CHO)], ***1a****, with [$ClCH_2PPh_3$)][Cl]/^{t}BuOK*

^{t}BuOK (0.12 g, 0.98 mmol) was added to a stirred suspension of [$ClCH_2PPh_3$][Cl] (0.33 g, 0.95 mmol) in toluene (10 mL) at 0 °C followed, after 30 min, by the dropwise addition of a solution of [Co(η^4-C_4Ph_4)(η^5-C_5H_4CHO)], **1a**, (0.47 g, 0.92 mmol) in toluene (10 mL). The mixture was warmed to room temperature and stirred for 24 h. After the addition of ^{t}BuOK (0.62 g, 5.0 mmol) the reaction mixture was refluxed for 1 h. The solvent was then removed under reduced pressure and the residue chromatographed on silica. Several products separated but only the *trans* complex *E*-[Co(η^4-C_4Ph_4)(η^5-C_5H_4–C≡C–CH=CH–C_5H_4-η^5)Co(η^4-C_4Ph_4)], *E*-**10a**, could be isolated and identified, its yield is very low.

2.8.1. E-[Co(η^4-C_4Ph_4)(η^5-C_5H_4–C≡C–CH=CH–C_5H_4-η^5)Co(η^4-C_4Ph_4)], ***E-10a***

^{1}H NMR ($CDCl_3$): δ 7.16–7.50 (40H, m, C_6H_5), 6.42 (1H, d, *J* = 16 Hz, C≡C–C*H*=CH), 6.25 (1H, d, *J* = 16 Hz, C≡C–CH=C*H*), 5.25 (2H, t, C_5H_4Co), 4.85 (2H, t, C_5H_4Co), 4.78 (2H, t, C_5H_4Co), 4.71 (2H, t, C_5H_4Co).

2.9. Crystal structure determinations

The structures of **2a**, **3a**, **4b**, **4a**, **5b**, *syn*-**6a**, *syn*-**6b** (2 crystal forms) and **7b** were determined by X-ray diffraction methods in the X-ray laboratory of University College Dublin. The data were collected at 100 K using a Bruker SMART APEX CCD area detector diffractometer and graphite-monochromated Mo Kα radiation (λ = 0.71073 Å). A full sphere of the reciprocal space was scanned by phi-omega scans. Pseudo-empirical absorption correction based on redundant reflections were made using SADABS [27]. The structures were solved by direct methods using SHELXS-97 [28] and refined by full matrix least-squares on F^2 for all data using SHELXL-97 [28]. For compounds **4a**, **5b**, *syn*-**6a** and **7b,** all hydrogen atoms were added at calculated positions and refined using a riding model. Their isotropic temperature factors were fixed to 1.2 times (1.5 times for methyl groups) the equivalent isotropic displacement parameters of the carbon/nitrogen atom the H-atom is attached to. For compounds **2a**, **3a**, **4b** and both polymorphs of *syn*-**6b**, all hydrogen atoms were located in the difference Fourier map and allowed to refine freely with isotropic temperature factors. Anisotropic temperature factors were used for all non-hydrogen atoms.

Calculations were carried out using ORTEX or Mercury [29]. Crystal structure data are given in Table 1a and 1b.

3. Results and discussion

The reactions carried out during the course of this work are summarized in Scheme 1. This includes the compound numbering where the [Co(η^4-C_4Ph_4)(η^5-C_5H_4R)] derivatives are **1a**, **2a** etc. whilst the corresponding [Fe(η^5-C_5H_5)(η^5-C_5H_4R] derivatives are **1b**, **2b** etc. These compounds are air-stable solids. They are soluble in the expected organic solvents to give coloured solutions which decompose slowly. In the text, the abbreviations Cb$^\varphi$ = Co(η^4-C_4Ph_4)(η^5-C_5H_4–) and Fc = Fe(η^5-C_5H_5)(η^5-C_5H_4–) are used.

Table 1a
Crystal data for **2a**.CH_2Cl_2, **3a**, **4a**, **4b** and **5b**.

Compound	**2a**.CH_2Cl_2	**3a**	**4a**	**4b**	**5b**
Empirical formula	$C_{36}H_{27}Br_2Cl_2Co$	$C_{35}H_{25}Co$	$C_{36}H_{25}CoO$	$C_{13}H_{10}FeO$	$C_{16}H_{10}FeN_2$
Formula weight	749.23	504.48	532.49	238.06	286.11
Temperature	100(2) K	100(2) K	100(2) K	100(2) K	100(2) K
Wavelength	0.71073 Å	0.71073 Å	0.71073 Å	0.71073 Å	0.71073 Å
Crystal system	Triclinic	Orthorhombic	Monoclinic	Orthorhombic	Monoclinic
Space group	P–1	Pna2_1	P2_1/c	P$2_12_12_1$	P2_1/c
Unit cell dimensions (Å), (°)	*a* = 10.2569(8) *b* = 11.7973(10) *c* = 13.1604(11) α = 102.253(1) β = 94.107(1) γ = 102.371(1)	*a* = 27.2299(16) *b* = 19.5624(12) *c* = 9.3332(6) α = 90 β = 90 γ = 90	*a* = 10.9417(9) *b* = 14.1524(11) *c* = 16.9912(13) α = 90 β = 97.515(1) γ = 90	*a* = 8.9159(6) *b* = 12.1183(8) *c* = 18.2166(12) α = 90 β = 90 γ = 90	*a* = 10.9971(17) *b* = 10.4508(16) *c* = 12.430(2) α = 90 β = 116.160(2) γ = 90
Volume (Å^3)	1508.6(2)	4971.6(5)	2608.5(4)	1968.2(2)	1282.2(3)
Z	2	8	4	8	4
Density calculated (Mg/m^3)	1.649	1.348	1.356	1.607	1.482
Absorption coefficient (mm^{-1})	3.420	0.713	0.686	1.495	1.160
F(000)	748	2096	1104	976	584
Crystal size (mm)	0.70 × 0.50 × 0.30	0.40 × 0.30 × 0.20	0.40 × 0.40 × 0.02	0.70 × 0.10 × 0.05	1.00 × 0.60 × 0.05
θ range for data collection	1.82–28.53°	1.82–28.55°	1.88–26.00°	2.02–25.99°	2.06–28.42°
Reflections collected	25786	41761	39253	30394	17508
Independent reflections	7040 [*R*(int) = 0.0238]	11679 [*R*(int) = 0.0366]	5129 [*R*(int) = 0.0335]	3858 [*R*(int) = 0.0241]	3064 [*R*(int) = 0.0260]
Completeness to θ max	91.8%	95.1%	100.0%	100.0%	94.9%
Absorption correction	Semi-empirical from equivalents	Semi-empirical from equivalents	Semi-empirical from equivalents	Semi-empirical from equivalents	Semi-empirical from equivalents
Max. and min. transmission	0.4269 and 0.2192	0.8706 and 0.7282	0.9864 and 0.7037	0.9290 and 0.7293	0.9443 and 0.6878
Refinement method	Full-matrix least-squares on F^2	Full-matrix least-squares on F^2	Full-matrix least-squares on F^2	Full-matrix least-squares on F^2	Full-matrix least-squares on F^2
Data/restraints/parameters	7040/0/370	11679/1/650	5129/0/443	3858/0/272	3064/0/212
Goodness–of–fit on F^2	1.036	1.026	1.100	1.082	1.061
Final *R* indices [I > 2sigma(I)]	*R*1 = 0.0249, w*R*2 = 0.0605	*R*1 = 0.0371, w*R*2 = 0.0849	*R*1 = 0.0376, w*R*2 = 0.0953	*R*1 = 0.0248, w*R*2 = 0.0650	*R*1 = 0.0265, w*R*2 = 0.0690
R indices (all data)	*R*1 = 0.0290, w*R*2 = 0.0619	*R*1 = 0.0425, w*R*2 = 0.0879	*R*1 = 0.0407, w*R*2 = 0.0974	*R*1 = 0.0262, w*R*2 = 0.0659	*R*1 = 0.0272, w*R*2 = 0.0697
Flack parameter	–	0.298(8)	–	0.50(2)	–
Largest diff. peak and hole (e.Å^{-3})	0.726 and –0.382	0.550 and –0.256	0.830 and –0.188	0.332 and –0.307	0.387 and –0.458

Table 1b
Crystal data for **6a**, **6b**.I, **6b**.II and **7b**.$CHCl_3$.

Compound	**6a**	*syn*-**6b**.(1)	*syn*-**6b**.(2)	*anti*-**7b**.$CHCl_3$
Empirical formula	$C_{42}H_{29}CoN_4O_4$	$C_{19}H_{14}FeN_4O_4$	$C_{19}H_{14}FeN_4O_4$	$C_{21}H_{17}Cl_3N_4O_4$
Formula weight	712.62	418.19	418.19	551.59
Temperature	100(2) K	100(2) K	100(2) K	100(2) K
Wavelength	0.71073 Å	0.71073 Å	0.71073 Å	0.71073 Å
Crystal system	Monoclinic	Monoclinic	Triclinic	Monoclinic
Space group	$P2_1/c$	Pn	P–1	$P2_1/c$
Unit cell dimensions (Å), (°)	a = 19.4991(19)	a = 5.9099(6)	a = 8.076(5)	a = 9.9905(7)
	b = 15.1097(15)	b = 14.0651(14)	b = 10.315(6)	b = 11.0671(8)
	c = 11.4831(11)	c = 10.4156(10)	c = 11.110(6)	c = 20.9881(15)
	α = 90	α = 90	α = 101.098(9)	α = 90
	β = 97.101(2)	β = 99.480(2)	β = 107.231(9)	β = 102.713(1)
	γ = 90	γ = 90	γ = 91.334(10)	γ = 90
Volume ($Å^3$)	3357.3(6)	853.96(15)	864.2(9)	2263.7(3)
Z	4	2	2	4
Density calculated (Mg/m^3)	1.410	1.626	1.607	1.618
Absorption coefficient (mm^{-1})	0.562	0.919	0.908	1.057
F(000)	1472	428	428	1120
Crystal size (mm)	0.30 × 0.30 × 0.01	1.00 × 0.40 × 0.01	0.18 × 0.18 × 0.15	0.50 × 0.30 × 0.20
θ range for data collection	1.71–26.00°	2.46–28.37°	1.96–26.00°	1.99–26.00°
Reflections collected	48976	12059	12587	34069
Independent reflections	6577 [R(int) = 0.0425]	3898 [R(int) = 0.0335]	3372 [R(int) = 0.0544]	4454 [R(int) = 0.0227]
Completeness to θ max	99.7%	94.2%	99.4%	100.00%
Absorption correction	Semi-empirical from equivalents	Semi-empirical from equivalents	Semi-empirical from equivalents	Semi-empirical from equivalents
Max. and min. transmission	0.9944 and 0.6743	0.9909 and 0.5628	0.8758 and 0.5062	0.8163 and 0.6716
Refinement method	Full-matrix least-squares on F^2	Full-matrix least-squares on F^2	Full-matrix least-squares on F^2	Full-matrix least-squares on F^2
Data/restraints/parameters	6577/0/576	3898/2/309	3372/0/309	4454/0/392
Goodness–of–fit on F^2	1.036	1.057	1.051	1.138
Final R indices [I > 2sigma(I)]	$R1$ = 0.0350, w$R2$ = 0.0859	$R1$ = 0.0358, w$R2$ = 0.0879	$R1$ = 0.0411, w$R2$ = 0.0943	$R1$ = 0.0380, w$R2$ = 0.0973
R indices (all data)	$R1$ = 0.0432, w$R2$ = 0.0897	$R1$ = 0.0367, w$R2$ = 0.0885	$R1$ = 0.0514, w$R2$ = 0.0989	$R1$ = 0.0389, w$R2$ = 0.0979
Flack parameter	–	0.081(14)	–	–
Largest diff. peak and hole (e.$Å^{-3}$)	0.493 and –0.189	0.509 and –0.245	0.957 and –0.263	0.717 and –0.471

The preparations of compounds **1a**, **3a**, and **1b**–**4b** have been reported previously and we have used similar but not always identical reactions to obtain them. Thus the method of Stevens and Richards was used to obtain [Cb$^{\varphi}$–CHO], **1a** [16], and that of Rosenblum [21] to obtain [Fc–CHO], **1b**. **1b** has been shown to react with the Ph_3P/CBr_4 reagent to give [Fc–CH=CBr_2], **2b**, which with ^{n}BuLi and then water affords [Fc–C≡CH], **3b** [30]. This reaction sequence, which was originally devised by Corey and Fuchs [31], was used to prepare **3a** via **2a** (as well as **3b** via **2b)** in preference to alternatives such as the dehydration of [Cb$^{\varphi}$–C(O)Me] (as available for the ferrocenylogue [32]) or the proven dehydrochlorination of [Cb$^{\varphi}$–CH=CHCl] [16]. Both **4a** and **4b** were prepared by the same method as that used previously to prepare **4b** [32] i.e. the deprotonation of the alkyne **3** with ^{n}BuLi and the reaction of the [Cb$^{\varphi}$–C≡C]$^{-}$ or [Fc–C≡C]$^{-}$ with Me_2NCHO. Hydrolysis of the mixtures gave [Cb$^{\varphi}$–C≡CCHO], **4a**, or [Fc–C≡CCHO], **4b**, in good overall yields.

4 underwent reactions which are typical of aldehydes and similar to those undergone by their precursors **1** [12,13]. Their base-catalysed Knoevenagel condensations with $CH_2(CN)_2$ [33] produced the deep red [Cb$^{\varphi}$–C≡C–CH=C(CN)$_2$], **5a**, or violet [Fc–C≡C–CH=C(CN)$_2$], **5b**. Their acid-catalysed condensations with 2,4-dinitrophenylhydrazine [34] gave the red hydrazones [Cb$^{\varphi}$–C≡C–CH=N–N(H)$C_6H_3(NO_2)_2$-2,4], **6a**, or [Fc–C≡C–CH=N–N(H)$C_6H_3(NO_2)_2$-2,4], **6b**, each as mixtures of *syn*- and *anti*-isomers (see Scheme 1); whereas only single isomers of orange [Cb$^{\varphi}$–C≡C–CH=N–N(Me)$C_6H_3(NO_2)_2$-2,4], **7a**, and [Fc–C≡C–CH=N–N(Me)$C_6H_3(NO_2)_2$-2,4], **7b**, were obtained from reactions with 1-methyl-1-dinitrophenylhydrazine. X-ray crystallography confirmed unambiguously **7b** as the *anti*- form and consistent spectroscopic data indicate the same for **7a**.

The reaction of **4a**/**b** with [Fe_2(η-C_5H_5)$_2$(CO)$_2$(μ-CO)(μ-CMe)][BF_4] [35] gave the highly coloured vinylcarbyne salts green-black [Fe_2(η-C_5H_5)$_2$(CO)$_2$(μ-CO)(μ-C–CH=CH–C≡C–Cb$^{\varphi}$)][BF_4], [**8a**][BF_4], and black [Fe_2(η-C_5H_5)$_2$(CO)$_2$(μ-CO)(μ-C–CH=CH–C≡C–Fc)][BF_4], [**8b**][BF_4].

Each of the reactions of **4** with the Wittig reagent [36] [Fc–CH_2PPh_3][I]/^{n}BuLi gave a mixture of the *E* and *Z* isomers of the but-1-ene-3-yne derivatives [Cb$^{\varphi}$–C≡C–CH=CHFc], **9a**, and [Fc–C≡C–CH=CHFc], **9b**, respectively. Although the isomers of **9b** could be separated, those of **9a** could not. Attempts to isomerise *Z*-**9a** to *E*-**9a** with I_2 were not successful as the iodine catalyst was consumed by the substrate. A similar reaction was attempted starting from [Cb$^{\varphi}$–CH_2PPh_3][Cl] [12], but its ylid failed to attack either **4a** or **4b**. These were recovered together with [Co(η^4-C_4Ph_4)(η^5-C_5H_4Me)] after the reaction mixtures were hydrolysed. Both *E* and *Z*-[Fc–C≡C–CH=CHFc], **9b**, have been prepared previously by the catalysed dimerisation [6a,6d,6e] of **3a**, but they were also formed as side-products of the reaction of [FcCHO] with [$ClCH_2PPh_3$][Cl]/^{t}BuOK in which the principal product was ferrocenylethyne **3b** [6b,6c], Attempts to prepare [Cb$^{\varphi}$–C≡C–CH=CHCb$^{\varphi}$], **10a**, from **1a** by a similar reaction gave a complex mixture of products from which was isolated *E*-**10a** (characterized by ^{1}H NMR spectroscopy) in very low yields. We recently reported the synthesis and X-ray crystal structure of [Cb$^{\varphi}$–C≡C–Ph] by the Castro-Stephens coupling [37] of **3a** and iodobenzene [19]. Various spectroscopic details and the electrochemistry of this compound are discussed in the following sections with those of compounds **3**–**9**.

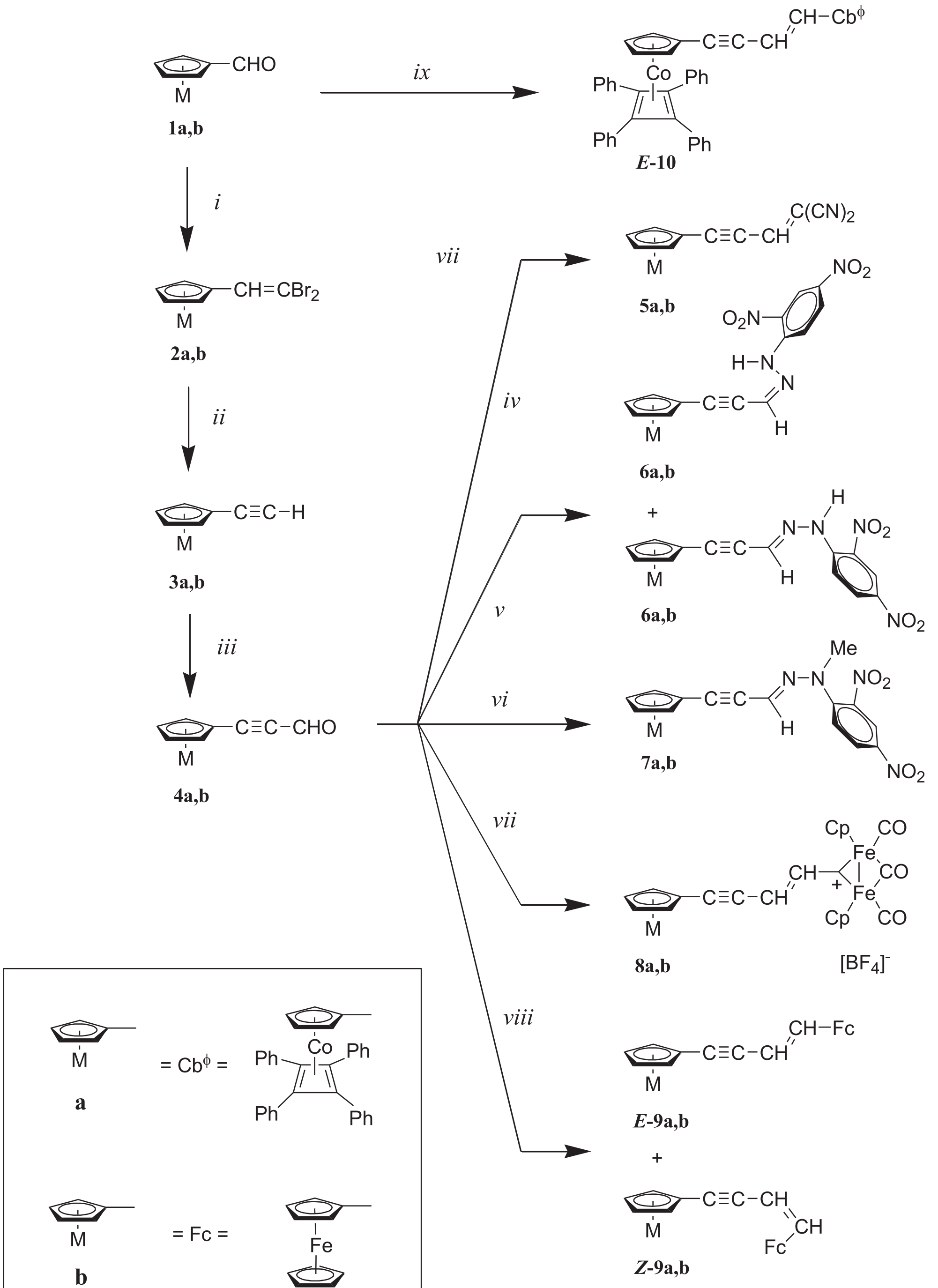

Scheme 1. (i) CBr_4/PPh_3. (ii) $^{n}BuLi$, then H_2O. (iii) $^{n}BuLi/HC(O)NMe_2$, then H_2O. (iv) $CH_2(CN)_2/Et_3N$. (v) 2,4–$(NO_2)_2C_6H_3N(H)NH_2/CH_3CO_2H$. (vi) 2,4-$(NO_2)_2C_6H_3N(Me)NH_2/CH_3CO_2H$. (vii) $[Fe_2(\eta^5\text{-}C_5H_5)_2(CO)_2(\mu\text{-}CO)(\mu\text{-}CCH_3)][BF_4]$, reflux. (viii) $[Fe(\eta^5\text{-}C_5H_5)(\eta^5\text{-}C_5H_4CH_2PPh_3)][I]/^{n}BuLi$. (ix) $[ClCH_2PPh_3)][Cl]/^{t}BuOK$ then further $^{t}BuOK$.

3.1. *Spectra*

3.1.1. *IR spectra*

The IR spectra of **3**–**9** all show absorption bands due to the internal vibrations of the Cb^{φ} and Fc moieties. Their frequencies do not vary greatly and they yield few structural or bonding insights, but they may obscure (e.g. two very strong bands at ca. 1498 and 1595 cm^{-1} characteristic of the η^4-C_4Ph_4 ligand) more important features.

However, the most interesting features of the IR spectra of the [Cb^{φ}–C≡C–X] and [Fc–C≡C–X] complexes **3**–**9** are the frequencies and intensities of the absorption bands due to their ν(C≡C) stretching vibrations. In general these are very sensitive to the substituents X and Z in Z–C≡C–X systems [38]. Those of our [Cb^{φ}–C≡C–X]/[Fc–C≡C–X] complexes are almost independent of Z (= Cb^{φ} and Fc), but their frequencies decrease for X = Ph (2214/2224, 2210) > *anti*-CH=N–N(Me)$C_6H_3(NO_2)_2$-2,4 (2207/2205 cm^{-1}) > *anti*-CH=N–N(H)$C_6H_3(NO_2)_2$-2,4 (2205/2203 cm^{-1}) > CH=CH–Fc-*Z* and *E* (2194/2194 cm^{-1}) > *syn*-CH=N–N(H)$C_6H_3(NO_2)_2$-2,4 (2184/2186 cm^{-1}) ≥ CHO (2181/2184 cm^{-1}) > CH=C(CN)$_2$ (2176/2175 cm^{-1}) » (CH=CH–C_{μ})(μ-

CO)(CO)$_2$Fe$_2$(η^5-C$_5$H$_5$)$_2^+$ (2148/2147 cm^{-1}) » H (2112/2110 cm^{-1}). X-ray diffraction studies (see below) show that the sole isomer of [**7b**] (X=CH=N–N(Me)C$_6$H$_3$(NO$_2$)$_2$-2,4) has the *anti*-conformation. Its ν(C≡C) frequency is very close to those of *anti*-[**6a**], *anti*-[**6b**] and *anti*-[**7a**], which suggests that the latter has the *anti*-conformation also. However, it is not immediately obvious why the *syn*-CH=NN(R)C$_6$H$_3$(NO$_2$)$_2$-2,4 end-groups are better π-acceptors than their *anti*-counterparts.

The intensities of the ν(C≡C) absorption bands also vary greatly with *X*. For example, in the solid state the intensity of the ν(C≡C) band of [Cb^{φ}–C≡C–Ph] [19] is ca. half of those due to the ν(C–H) vibrations of its C$_4$Ph$_4$ groups. In contrast, for [Cb^{φ}–C≡C–CHO] the intensity of the ν(C≡C) band has increased by ca. 6400% using the same measure. This may be a consequence of the permanent dipole induced across the C≡C bond by its substituents. As Cb^{φ} and Fc are donor groups of similar though not identical capabilities, the magnitude of this permanent dipole will largely be a function of the acceptor strength of X in **3**–**9**. The larger it is, the greater will be the dipole gradient change during the ν(C≡C) vibration and the more intense will be the resultant IR absorption band. However, this is not the whole story. When the IR spectra of [Cb^{φ}–C≡C–CHO], **4a**, and [Cb^{φ}–C≡C–CH=C(CN)$_2$], **5a**, are compared, the ν(C≡C) and ν(C=C) bands of the latter are weaker than the ν(C≡C) and ν(CO) bands of the former [Relative peak heights ν(C–H$_{Ph}$):ν(C≡C):ν(C=O) or ν(C=C) = 1:34:41 for **4a** and 1:10:5 for **5a**.] whilst on some measures the CH=C(CN)$_2$ group is more electron-withdrawing than the CHO. This may be explained if it is assumed that the ν(C≡C) vibration of **4a**, as well having a large intrinsic dipole gradient change, also mixes with the ν(C=O) vibration and "borrows" intensity from it. On the other hand the ν(C=C) vibration of **5a** only gives a relatively weak absorption band, so any mixing of this with the ν(C≡C) mode is likely to result in "intensity transfer" *from* rather than *to* the latter, and a weaker absorption band at ca. 2160 cm^{-1}. Such coupling between the ν(C≡C) vibrations and those of its substituents has been shown to be very important for terminal alkynes. The consequences of replacing the terminal ≡CH of Ph–C≡CH by ≡CD or ≡CMe are best explained by assuming coupling between ν(C≡C) and ν(C–H)/ν(C–D) vibrations which greater for Ph–C≡CD than for Ph–C≡CH [39–41] and which disappears in Ph–C≡CMe [42]. Thus for the terminal alkynes **3a**/**3b** the ν(C≡C) are 2112/2110 cm^{-1} with ν(CC–H) at ca. 3302/3302 cm^{-1}, whereas for the alkynyl aldehydes **4a**/**4b** ν(C≡C) are 2184/2181 cm^{-1}. A similar increase is observed in other terminal *vs.* internal alkynes e.g. [Ni(η^5-C$_5$H$_5$)(PPh$_3$)C≡CH]/[Ni(η^5-C$_5$H$_5$)(PPh$_3$)C≡CPh] ν(C≡C) = 1958/2099 cm^{-1} [14c] or [PhC≡CH]/[PhC≡CCHO] where ν(C≡C) = 2110/2190 cm^{-1}. It is coupling between ν(CC–H) and ν(C≡C) vibrations which increase the frequencies of the former and depresses the frequencies of the latter. In the solid state spectrum of **4a**, there are two absorption bands due to its ν(CC–H) vibration; in that of **4b** there are three which has been attributed to intermolecular C≡C–H···C≡C interactions [43]. The IR of both compounds in solution show a single band due to their ν(C–H) modes. This is discussed in more detail in Section 3.2.

The ν(CO) vibrations of the aldehyde groups of **4a** and **4b** give rise to strong absorption bands at 1649 and 1648 cm^{-1} respectively. These compare with 1683 and1687 cm^{-1} observed for **1a** and **1b**. The interpolation of a C≡C spacer also causes a decrease in the ν(CO) frequency from PhCHO (1709 cm^{-1}) to PhC≡CCHO (1661 cm^{-1}) [38,42]. The CN groups of **5a**/**5b** give rise to quite weak absorption bands at 2224/2230 cm^{-1} compared with 2220/2185, 2170 cm^{-1} for [Cb^{φ}–CH=C(CN)$_2$]/[Fc–CH=C(CN)$_2$] [12,44]. The nitro groups in **6** and **7** give rise to readily identified absorption bands at ca. 1340 and 1520 cm^{-1}, and another weak band at ca.1600 cm^{-1} is assigned tentatively to their ν(C=N) modes. This is not always detected. These frequencies are comparable to those found for [Cb^{φ}–CH=N–N(H)C$_6$H$_3$(NO$_2$)$_2$-2,4] at 1336, 1518 and 1616 cm^{-1} respectively [12].

There are very strong absorption bands in the IR spectra of **8a** (2033, 2004 and 1848 cm^{-1}) and **8b** (2033, 1996 sh, 1844 cm^{-1}) which are assigned respectively to the symmetric ν(CO$_t$), anti-symmetric ν(CO$_t$) and ν(CO$_\mu$) vibrations of their *cis*-Fe$_2$(η-C$_5$H$_5$)$_2$(CO)$_2$(μ-CO)(μ-C–) moieties. Their frequencies suggest that both the –CH=CH–C≡C–Cb^{φ} and –CH=CH–C≡C–Fc moieties act as electron donors to the cationic diiron acceptor endgroup (for [Fe$_2$(η-C$_5$H$_5$)$_2$(CO)$_2$(μ-CO)(μ-CCH$_3$)]$^+$[BF$_4$]$^-$ ν(CO) = 2046, 2012, 1853 cm^{-1}), but that Fc is marginally stronger than Cb^{φ}. When the frequencies for **8b** are compared with those for [Fe$_2$(η-C$_5$H$_5$)$_2$(CO)$_2$(μ-CO)(μ-C–(CH=CH)$_n$-Fc]$^+$ {ν(CO) = 2024, 1993, 1837 when $n = 1$; 2027, 2001, 1837 cm^{-1} when $n = 2$} [15c] it can be seen that the donor effect of the ferrocenyl (and presumably of Cb^{φ}) on the Fe$_2$(η-C$_5$H$_5$)$_2$(CO)$_2$(μ-CO)(μ-C$^+$) group is reduced when –C≡C– is introduced between Fc- and Fe$_2$(η-C$_5$H$_5$)$_2$(CO)$_2$(μ-CO)(μ-C–C=CH–) whereas the introduction of –CH=CH– has a much more limited effect i.e. C≡C hinders donor→acceptor communication in D-π-A systems more than CH=CH. This poorer conjugation through an alkyne spacer has been noted previously [45]. The spectra of **8a** and **8b** also show strong absorption bands at ca.1150 cm^{-1} due to the [BF$_4$]$^-$ ions.

3.1.2. ^{1}H NMR spectra

As expected, the ^{1}H NMR spectra of **1a**–**8a** all show two pseudo-triplets due to their η^5-C$_5$H$_4$ ligands (δ 4.60–5.12 with J = ca. 2 Hz) together with a multiplet due the phenyl groups of the η^4-C$_4$Ph$_4$ ligands (δ 7.11–7.50). Their ferrocenyl counterparts similarly show the two (η^5-C$_5$H$_4$) pseudo-triplets (δ 4.21–4.78 with J = ca. 2 Hz) and the unsubstituted (η^5-C$_5$H$_5$) ligand singlet (δ 4.19–4.44). In comparable compounds the C$_5$H$_4$ signals of the Cb^{φ} group lie at higher δ than those of the Fc group. The chemical shifts of the various protons are comparable with those observed for similar compounds such as [Cb^{φ}–C≡C–Ph], [Fc–C≡C–R], [Cb^{φ}–CH=CH–R] and *E*-[Fc–CH=CH–R] (R = aryl) [9,13,19].

With the exception of [Cb^{φ}–C≡C–H] and [Fc–C≡C–H], the terminal groups have the general formula –CH=Y and for them the chemical shifts δ of the singlets due to the C≡C–C*H*=Y protons is always greater in the ferrocenyl complexes than their Cb^{φ} counterparts. It is also a function of Y and increases –CH=Y = –CH=CH– < –CH=N– < –CHO for both Cb^{φ} and Fc derivatives.

The N-*H* resonances of *Z* and *E* isomers of both **6a** and **6b** are relatively sharp and highly deshielded with δ 11–12.5 compared with the more normal δ 7–8. This has also been observed for [Cb^{φ}–CH=N–N(H)C$_6$H$_3$(NO$_2$)$_2$-2,4] and is probably due to intramolecular hydrogen bonding between NH and NO$_2$ groups which is found in the solid state and retained in solution. In **7a**/**7b** it is replaced by Me singlets at δ 3.73/3.26 respectively.

There are three signals in the spectra of [**8a**][BF$_4$]/[**8b**][BF$_4$] which are characteristic of the Fe$_2$(η-C$_5$H$_5$)$_2$(CO)$_2$(μ-CO)(μ-C–CH=CH–)$^+$. The first is a singlet (10H) at δ 5.35 due to (η^5-C$_5$*H*$_5$)$_2$Fe$_2$ and its singlet nature confirms that, although the CH=CH–C≡C moiety probably lies in the Fe$_2$C$_\mu$ plane (cf. [Fe$_2$(η-C$_5$H$_5$)$_2$(CO)$_2$(μ-CO){μ-C–C(Cl)=CH–Fc}][BF$_4$] [15c]), there is rapid rotation about the C$_\mu$–C bond. The other two signals are doublets at δ 8.92/9.35 (1H) and δ 6.58/6.96 (1H) due to the C$_\mu$–C*H*$_a$=C*H*$_b$– protons respectively; their coupling constants (ca. 14 Hz) confirm their *E* relationship.

The *Z* and *E* isomers of [Co(η^4-C$_4$Ph$_4$)(η^5-C$_5$H$_4$–C≡C–CH=CH–C$_5$H$_4$-η^5)Fe(η^5-C$_5$H$_5$)], **9a** and [Fe(η^5-C$_5$H$_5$)(η^5-C$_5$H$_4$–C≡C–CH=CH–C$_5$H$_5$-η^5)Fe(η^5-C$_5$H$_5$)], **9b**, can be distinguished by their –C*H*=C*H*– coupling constants of 11–12 Hz and 16 Hz respectively. Because pure samples of both *Z* and *E*-**9b** could be obtained, attribution and assignment of the signals in their ^{1}H NMR spectra is relatively straightforward [6c]. However, this is not the case for **9a** where the *Z* and *E* isomers were formed in ca. equal amounts and could not be separated. However, a near-complete assignment of the spectrum has been made by using correlation spectroscopy and comparisons with the spectra of *Z*-**9b** and *E*-**9b**. We are confident of that for the $C{\equiv}C{-}CH{=}CH{-}C_5H_4{-}\eta^5)Fe(\eta^5{-}C_5H_5)$ parts of both *Z* and *E*-**9a** but rather less so of that for the $Co(\eta^4{-}C_4Ph_4)(\eta^5{-}C_5H_4{-})$ end-group. However, assignments are consistent with related Cb$^{\varphi}$ and Fc substituted alkene and alkyne systems [9,13,19].

3.1.3. ^{13}C NMR spectra

The spectra were assigned by using homo and heteronuclear 2-D NMR techniques, internal consistency and by comparisons with related compounds. The spectra of all Cb$^{\varphi}$ complexes show one signal due to the cyclobutadiene carbon atoms (ca. δ 77), four for the Ph groups of the η^4-C_4Ph_4 ligand, and three resonances due to their $Co(\eta^5{-}C_5H_4)$ groups. This confirms that rotations of the C_4 and C_5 ligands about their centroid–Co axes and of the phenyl groups about the C–Ph axes are fast on the NMR timescale. As expected, the spectra of the Fc complexes show three signals due to the η^5-C_5H_4 ligands and a η^5-C_5H_5 singlet, and closely resemble those of other ferrocenyl alkynes. In all comparable pairs of compounds δ $C_5H_4Co > \delta$ C_5H_4Fe.

The spectra of **3**–**10** show two signals due to their acetylenic C atoms $C_5H_4C{\equiv}C$-X. Their chemical shifts lie in the range δ 78–104 for the Cb$^{\varphi}$ complexes and δ 71–108 for the Fc derivatives.

The resonances due to the terminal groups X are readily assigned for **4a**/**4b** when X = *C*HO at δ 176.6/176.3 respectively. These are less deshielded than those of the aldehydes [Cb$^{\varphi}$–*C*HO]/[Fc–*C*HO] (δ 191.0/193.9) or [Ph–*C*HO] at δ 192.3 [42]. The *C*H=C(CN)$_2$ resonance of the dicyanoethene derivatives **5a**/**5b** (δ 142.0/141.4) are similarly shielded compared with [Cb$^{\varphi}$–*C*H=C(CN)$_2$] (δ 157.4). Their *C*(*C*N)$_2$ signals are found within the typical range δ 120–113.0 [14a]. The –*C*H=N-N(H)$C_6H_3(NO_2)_2$-2,4 atoms of *syn*- and *anti*-**6a**/**6b** are unremarkable, but display clear similarities between Cb$^{\varphi}$ and Fc variants, yet similarly distinct differences for the *syn*- and *anti*-forms. Taken together these suggest an *anti*-configuration for the single isomeric forms obtained of **7a**/**7b**.

Of particular interest in the spectrum of [**8a**][BF$_4$] are the signals due to the Cμ, μ-CO and t-CO ligands of the $Fe_2(\mu{-}C\mu)(\mu{-}CO)(t{-}CO)_2$ fragment at δ 436, 254 and 209 ppm respectively. The chemical shifts of all three, though high, are normal for this class of compound and compare with those found in $[Fe_2(\eta{-}C_5H_5)_2(CO)_2(\mu{-}CO)(\mu{-}C_\mu{-}CH{=}CH{-}CH{=}CH{-}Fc][BF_4]$ (δ 411, 257, 209) and $[Fe_2(\eta{-}C_5H_5)_2(CO)_2(\mu{-}CO)(\mu{-}C{-}CH_3][BF_4]$ (δ 499, 272, 206) [15c]. The single signals due to η^5-C_5H_5 and t-*C*O ligands confirm that rotation about the μ-Cμ–CH bond is fast on the NMR timescale.

The spectra of *E* and *Z*-**9b** are readily assigned; that of the inseparable *E* and *Z*-**9b** is not. As for the ^{1}H NMR spectrum, we are confident of the attribution and assignment of signals due to the $({-}C{\equiv}C{-}CH{=}CH{-}C_5H_4{-}\eta^5)Fe(\eta^5{-}C_5H_5)$ part of both *Z* and *E*-**9a** but less so of that for the $Co(\eta^4{-}C_4Ph_4)(\eta^5{-}C_5H_4{-})$ end-group. The chemical shifts of the various C atoms are comparable with those observed for similar compounds such as Cb$^{\varphi}$–C≡C–Ph, Fc–C≡C–R, Cb$^{\varphi}$–CH=CH–R and *E*-Fc–CH=CH–R (R = aryl) [9,13,19].

3.1.4. UV–Vis spectra

The electronic spectrum of [Fc–C≡C–H], **3b**, shows a strong peak at 269 nm and weaker ones at (i) 329 and (ii) 443 nm. Counterparts of the latter two are observed in the spectra of other ferrocenyl derivatives and have been attributed to transitions essentially metal-centred within the $Fe(\eta^5{-}C_5H_5)(\eta^5{-}C_5H_4)$ moiety. Similar bands are observed in the spectrum of [Cb$^{\varphi}$–C≡C–H] at 318 and 392 nm and assumed to have similar causes. When H is replaced by an acceptor group assignment of the electronic spectral bands becomes non-trivial, as formerly metal-based transitions take on increasing ligand character, or are supplemented or masked by other chromophores within the molecule. For **4**–**8**, in all cases the long-wavelength absorption maxima of the Fc compounds appears at lower energy than the analogous Cb$^{\varphi}$ example, suggesting the ferrocenyl is a better donor. However, apart from this observation, and despite the availability of electronic spectral data of M–CH=Y for most of the M–C≡C–CH=Y reported here [12,15c,44,46], it is difficult to draw firm conclusions on the nature of the long-wavelength λ_{max} absorption band and its relationship to the strength of the acceptor. As an example, insertion of an alkyne into Cb$^{\varphi}$–CHO shifts λ_{max} from 422 nm to higher energy at 392 nm in **4a**. A similar hypsochromic shift occurs for **5a** cf. Cb$^{\varphi}$–CH=C(CN)$_2$. For the ferrocenyl compounds **4b**, **5b** and **8b** however, λ_{max} shifts bathochromically compared with the analogous compound without the alkyne extension. Within each M–C≡C–CH=Y series λ_{max} increases as the acceptor strength of CH=Y increases CHO < CH=C(CN)$_2$ < $({-}CH{=}CH{-}C_\mu^+)(\mu{-}CO)(CO)_2Fe_2(\eta^5{-}C_5H_5)_2$. Thus the lowest energy absorptions of Fc–C≡C–CH=Y, **4b**, **5b** and **8b** appear at 468, 560 and 722 nm respectively. We note that these are at slightly shorter wavelength than their equivalent Fc–CH=CH–CH=Y [15c,47,48] confirming again that conjugation is more effective through –CH=CH– than through –C≡C–. Both **5a**/**b** and **8a**/**b** display relatively uncommon negative solvatochromism [49] although this effect has been previously observed with the diiron end group [15c]. For these complexes the ground state is more polar than the electronic excited state and solvation in a higher polarity solvent sees λ_{max} shift to higher energy.

For characterization of aldehydes, 2,4-dinitrophenylhydrazones are probably the most important derivatives. Of these the *anti*- (or *E*-) isomer is generally the most stable, but acidity or UV-light can cause conversion to the *syn*- (*Z*-) form [50]. Often in the literature however the form characterized is unspecified [14a,51], which makes analysis of our spectral data more difficult. For **6a** and **6b** the long-wavelength absorption band of the *anti*- form is at lower energy than the *syn*-, a result in keeping with the predicted extra stability of the *anti*- mentioned above. In context with the rest of this work and the focus on D-π-A behaviour, the phenyl hydrazones do not fit clearly in sequence with **4**, **5** and **8**. The spectral bands of *syn*- and *anti*- isomers of **6a** are shifted bathochromically with respect to their relatives without the alkyne spacer [12], and both **6a** and **6b** display the more common positive solvatochromism.

The spectrum of the mixed **9a** isomers is essentially, the sum of the $Co(\eta^4{-}C_4Ph_4)(\eta^5{-}C_5H_4{-})$ and $Fe(\eta^5{-}C_5H_5)(\eta^5{-}C_5H_4{-})$ chromophores. The separable *E* and *Z* forms of **9b** differ only in detail in the UV portion of electronic spectrum, an extra band at 284 nm observed for the cis form.

3.2. Molecular structures

X-ray crystallography has been used to determine the crystal and molecular structures of four Cb$^{\varphi}$ complexes and four Fc derivatives. Crystal data are given in Tables 1 and 2. The structures are illustrated in Fig. 1 (**3a**), Fig. 2 (**4a**), Fig. 3(**4b**), Fig. 4 (**5b**), Fig. 5 (*syn*-**6a**), Fig. 6 (*syn*-**6b** Structure 1), Fig. 7 (*anti*-**7b**) and Fig. 8 (**2a**); these also include the atom labeling.

The structure of **3a**, $[Co(\eta^4{-}C_4Ph_4)(\eta^5{-}C_5H_4C{\equiv}CH)]$ (Fig. 1), has been reported previously but with an “unrealistically short” C≡C bond length [17]. Our crystal appears to have the same morphology as that used by Classen et al. though with slightly different unit cell dimensions, and data collection was carried out at 100 K rather than 200 K. In this case both of the independent molecules in the

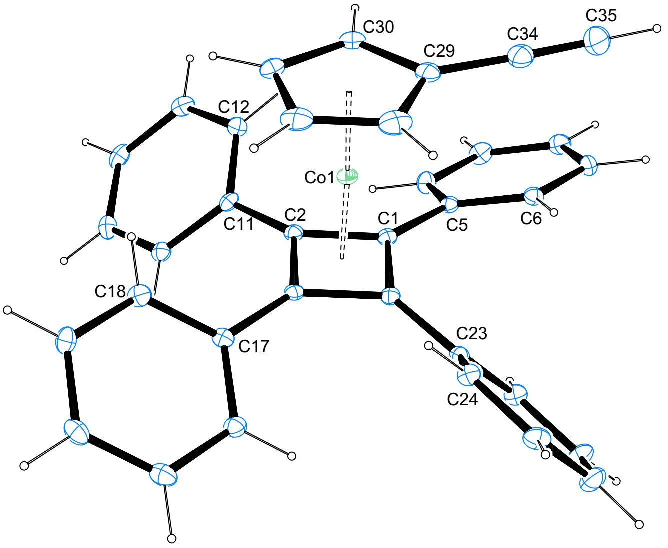

Fig. 1. Molecular structure and atom numbering for [Co(η^4-C_4Ph_4)(η^5-C_5H_4–C≡C–H)], **3a** (molecule 1). Thermal ellipsoids in this and following figures are drawn at the 50% probability level, and for clarity only the first two C atoms of consecutively numbered aromatic rings are numbered. Selected bond lengths (Å) for molecule 1 {molecule 2}, Co–C_5H_4(cent) 1.671 {1.684}; Co–C_4Ph_4(cent) 1.690 {1.689}; C29–C34 1.431(3) {1.427(3)}; C34–C35 1.191(4) {1.188(3)}. Selected bond angles (°) for molecule 1 {molecule 2}, C29–C34–C35 178.1(3) {178.1(3)}; C_5H_4(cent)-Co-C_4Ph_4(cent) 177.1 {171.8}.

asymmetric unit gave more reasonable C≡C distances which are consistent with those reported for Cb^{φ}–(C≡C)$_n$–R (n = 2) [17]. There are also two independent molecules in the unit cell of **4b**, whilst the η^5-C_5H_5 ligand of *anti*-**7b** is disordered over two sites. Two different crystal forms of *syn*-**6b** were obtained and shown to have similar but not identical molecular structures; only one is illustrated (Fig. 6).

All the alkyne complexes are shown to have the expected structures in which a C_5H_4–C≡C–X ligand is η^5 bonded through its C_5H_4 group to a Co(η^4-C_4Ph_4) or Fe(η^5-C_5H_5) fragment. The planar C_5H_4/C_4Ph_4 rings of Cb^{φ} complexes and C_5H_4/C_5H_5 rings of ferrocenes are parallel or close to it with interplanar angles of 1.2–5.5° and centroid–M–centroid angles of 174.4(1)–179.6(1)° (Average = 178°). The two C_5 ligands are eclipsed or close to it in **4b**, *syn*-**6b** (Structure 2) and the major disorder component of *anti*-**7b** (C1A–C5A); and they deviate from the ideal eclipsed arrangement by 7.5° in **5b** and 18.9° in *syn*-**6b** (Structure 1). The minor disorder component (28%) of *anti*-**7b** (C1B - C5B) is staggered.

As in all Cb^{φ} complexes, the η^4-C_4Ph_4 group does not have its Ph groups lying in the C_4 plane [10c,12,13,17,19]. The C–Ph bonds point away from the Co atoms with ring centroid-C–Ph angles of 169–178° thus resembling a four-legged piano stool. Additionally the tilted Ph rings constitute a four-bladed propeller with an average angle between the C_4 and Ph planes of 37°. Compound **6a** contains both the minimum (18.9°) and maximum tilt (73.3°) examples on adjacent C_4 carbons. In the case of the latter, ring geometry is such that there are two edge-to-face C–H···π interactions, in the former, the geometry allows (or is determined by) a C–H···O hydrogen bond with augmentation from both C–H···π(alkyne) and C–H···π(ring) interactions. These results suggest that the individual ring tilt, *i.e.* spatial arrangement of the phenyls, is principally a function of crystal packing effects. Although the four-bladed propeller arrangement is inherently chiral, the solid state molecules pack in the unit cell in symmetry generated *rac* pairs. In solution the chirality is not maintained due to rotation of the phenyl groups.

In the Cb^{φ} complexes the average Co–C_4 centroid [1.690(1) Å] and Co–Cp centroid [1.68(1) Å] distances, and C–C bond lengths within the C_4 and C_5 rings are comparable with those previously reported. Within the C_5H_4 ligand there is a subtle elongation of the two $C_{i(pso)}$–C compared with the other three C–C bonds. Bond lengths within the ferrocenyl fragments are similarly unremarkable.

In most complexes the (C_5 centroid)–C_i–C_α≡C_β–X atom sequence is close to linear with average angles of 178.0, 178.1 and 177.7° for centroid–C_i–C_α, C_i–C_α≡C_β and C_α≡C_β–X respectively. The exception to this is *anti*-**7b** where C_α≡C_β–X is 168.7(2). The C_α

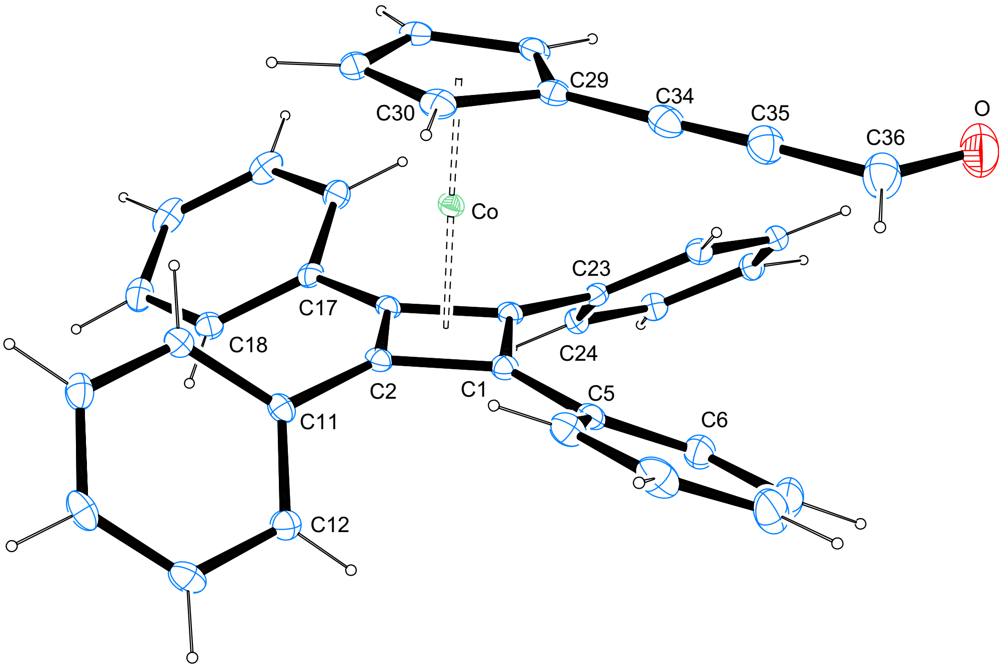

Fig. 2. Molecular structure and atom numbering for [Co(η^4-C_4Ph_4)(η^5-C_5H_4–C≡C–CHO)], **4a**. Selected bond lengths (Å), Co-C_5H_4(cent) 1.677; Co-C_4Ph_4(cent) 1.691; C29–C34 1.418(3); C34–C35 1.211(3); C35–C36 1.424(3). Selected bond angles (°), C29–C34–C35 178.1(3); C34–C35–C36 176.8(2); C_5H_4(cent)-Co-C_4Ph_4(cent) 178.0.

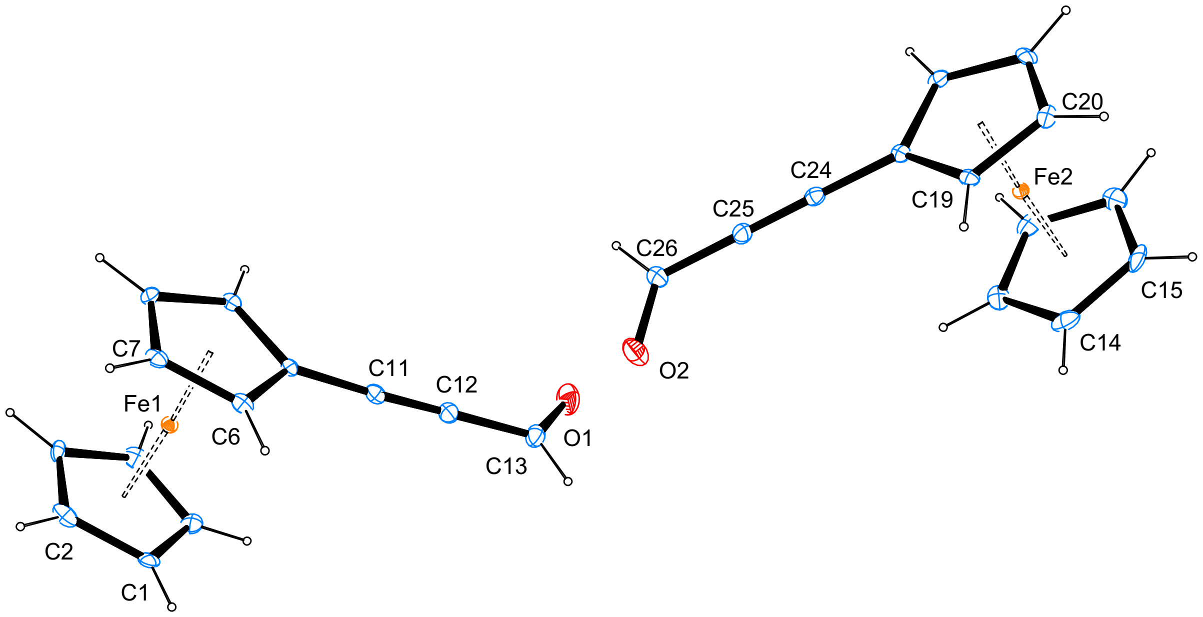

Fig. 3. Molecular structure and atom numbering for [Fe(η^5-C_5H_5)(η^5-C_5H_4–C≡C–CHO)], **4b** (asymmetric unit). Selected bond lengths (Å) for molecule 1 {molecule 2}, Fe–C_5H_4(cent) 1.646 {1.643}; Fe–C_5H_5(cent) 1.655 {1.646}; C10–C11 1.415(2) {1.419(2)}; C11–C12 1.205(3) {1.206(3)}; C12–C13 1.436(3) {1.431(3)}; O1···H26 3.258(2); O2···H13 2.756(2). Selected bond angles (°) for molecule 1 {molecule 2}, C10–C11–C12 177.4(3) {178.0(3)}; C11–C12–C13 177.7(4) {177.7(3)}; C_5H_4(cent)-Fe-C_5H_5(cent) 176.9 {177.1}.

atoms do not always lie in the C_5H_4 plane but may be displaced from it towards or away from Co/Fe by up to 0.086 Å. There is no apparent pattern to this; e.g. in molecule 1 of **3a** it is 0.064 Å away from Co, but in molecule 2 it is 0.007 Å. C_β behaves similarly but the displacements are usually greater, 0.011–0.179 Å. Again we suggest that the subtle differences observed are the result of crystal packing interactions.

The C_i–C_α, C_α≡C_β and C_β–C_x bond lengths lie in the ranges 1.413(2) – 1.431(3) Å, 1.188(3)–1.211(3) Å and 1.404(2) – 1.436(3) Å respectively, and are similar for Cb$^\varphi$ and Fc derivatives. These bond lengths are comparable with those found in organic [52] and organometallic alkynes such as [Fc–C≡CPh] [53], [Fc–C≡C–C≡C–Fc] [6c], [Fc–C≡C–pyrenyl-1] [9] and [Cb$^\varphi$–C≡C–C≡C–Cb$^\varphi$] [17].

Although the terminal groups X in **3a** and **3b** are hydrogen atoms, in all other alkyne structures described here it is a ca. planar –CH=Y moiety based on a sp^2 hybridised C atom which is ca. coplanar with the C_5H_4 group (interplanar angle = 0–19.6°) e.g. in the alkynyl aldehydes **4a** and **4b** (Y=O) the angles between the C_5H_4 and C_βCHO planes are 12.6° and 4.2/16.8° respectively, and in **5b** that with C_βCH=C(CN)$_2$ is 4.5°. This contrasts with the situation in [Fc–C≡C–aryl] complexes [9,53] where the C_5H_4 and aryl planes of the (η^5-C_5H_4–C≡C–aryl) ligand are orthogonal or close to it, and in [Cb$^\varphi$–C≡C–C_6H_5] where the corresponding angle is 34.92(18)° [19].

In both **3a** and **3b**, the terminal group X = H. A previous X-ray diffraction study on [Fc–C≡C–H], **3b** [43] shows that in the solid state it forms trimeric units held together by weak interactions

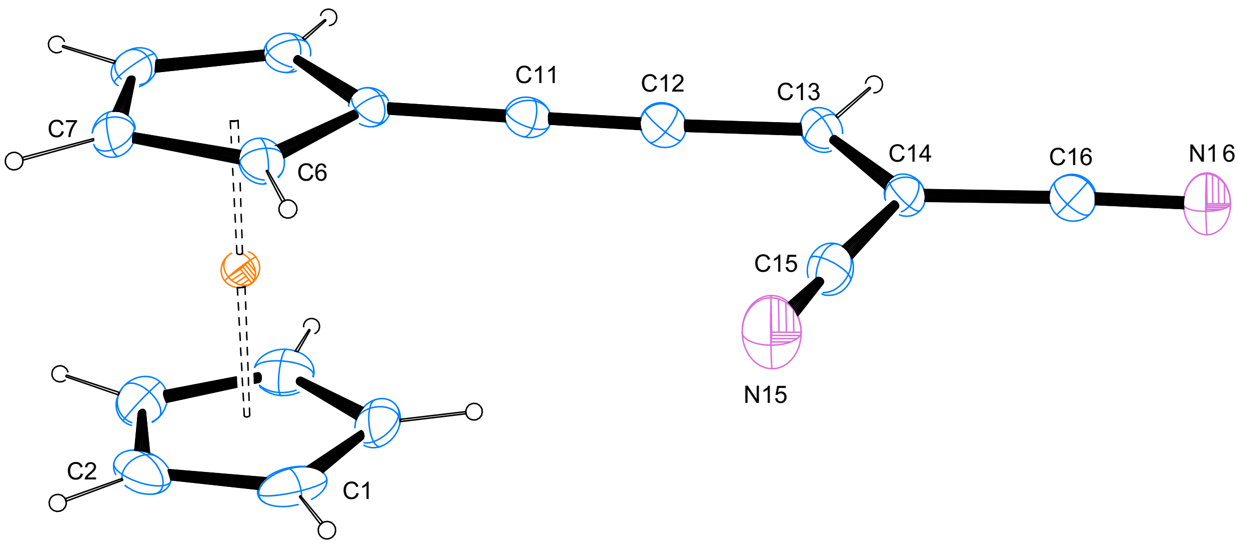

Fig. 4. Molecular structure and atom numbering for [Fe(η^5-C_5H_5){η^5-C_5H_4–C≡C–CH=C(CN)$_2$}], **5b**. Selected bond lengths (Å) Fe–C_5H_4(cent) 1.645; Fe–C_5H_5(cent) 1.625; C10–C11 1.415(2); C11–C12 1.206(3); C12–C13 1.404(2); C13–C(14 1.357(2). Selected bond angles (°) C10–C11–C12 178.53(11); C11–C12–C13 1.7832(13); C12–C13–C14 122.93(11); C_5H_4(cent)-Fe-C_5H_5(cent) 179.1.

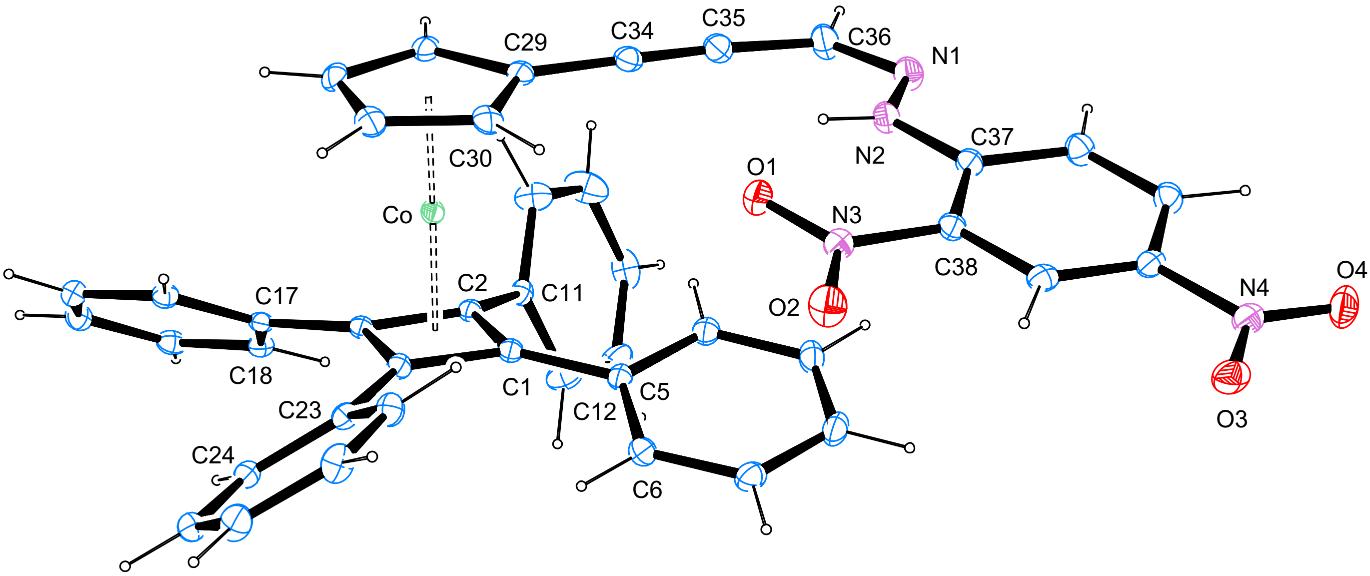

Fig. 5. Molecular structure and atom numbering for *syn*-[Co(η^4-C_4Ph_4)[η^5-C_5H_4–C≡C–CH=N–$NHC_6H_3(NO_2)_2$-2,4], *syn*-**6a**. Selected bond lengths (Å), Co–C_5H_4(cent) 1.674; Co–C_4Ph_4(cent) 1.691; C29–C34 1.420(2); C34–C35 1.203(3); C35–C36 1.417(3); H2N···O1 2.001(17). Selected bond angles (°), C29–C34–C35 179.0(2); C34–C35–C36 175.77(19); N2–H···O1 132(4); C_5H_4(cent)-Co–C_4Ph_4(cent) 175.7.

between the terminal H of one molecule and the C≡C of a neighbour with $H\cdots C_{\alpha,\beta} = 2.69–3.45$ Å. All three interactions within the trimers are different and each gives rise to a separate ν(C–H) absorption band in the solid state IR spectrum at 3276, 3289 and 3295 cm^{-1}. In CCl_4 solution a single band is observed at 3311 cm^{-1}. For [Cb^{φ}–C≡C–H], **3a** there are two independent molecules in the asymmetric unit and two ν(CC–H) absorption bands in the solid state IR spectrum at 3305 and 3275 cm^{-1}; the 'typical' value for a 'free' ν(≡C–H) vibration is ca. 3311 cm^{-1}. The shortest nonbonded distances involving C≡C–*H35* in molecule 1 are 3.04 to C69 (molecule 2) and 3.14 Å to C25 (an adjacent molecule 1). There is a genuine C–H···π contact (2.95 Å) involving C≡C–*H70* (molecule 2) to the centroid of the C23–C28 phenyl ring in molecule 1. It is possible that ν(C–H70) is responsible for the more shifted absorption band at 3275 cm^{-1} whilst the much more weakly interacting C≡C–H35 is responsible for the scarcely shifted 3305 cm^{-1} band. In **4a** there are short contacts (3.333 Å) between the terminal aldehyde H and a proximal alkyne centroid generating an inversion related dimer. In the ferrocenyl complex **4b**, dimers are formed by a 6-membered ring motif involving two C(H)O···HC(O) interactions between adjacent molecules 1 and 2. The two H···O distances are different at 3.258 and 2.756 Å.

For the hydrazones, **6**, where the –CH=Y termini are –CH=N–N(H)$C_6H_3(NO_2)_2$-2,4, although *syn*- and *anti*-isomers were prepared only the *syn*-form of **6a** (Fig. 5) provided X-ray quality crystals. Similarly only dimorphs of the *syn*-**6b** (Fig. 6) were characterised. As is usual for such hydrazones, there is intramolecular =N–N–H···ON(O) hydrogen bonding with H···O distances/N–H···O

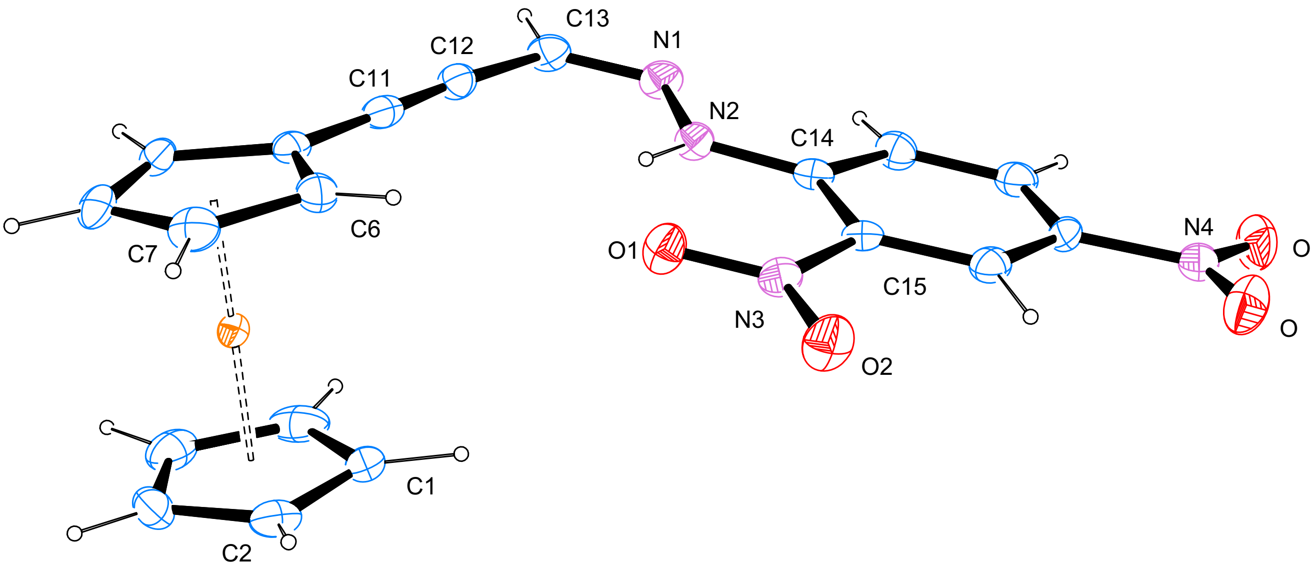

Fig. 6. Molecular structure and atom numbering for *syn*-[Fe(η^5-C_5H_5){η^5-C_5H_4–C≡C–CH=N–N(H)$C_6H_3(NO_2)_2$-2,4}], *syn*-**6b** (structure 1 illustrated). Selected bond lengths (Å) for structure 1 {structure 2}, Fe–C_5H_4(cent) 1.644 {1.644}; Fe–C_5H_5(cent) 1.657 {1.649}; C10–C11 1.421(4) {1.430(4)}; C11–C12 1.204(4) {1.196(4)}; C12–C13 1.418(4) {1.420(4)}; HN2···O1 1.91(4) {2.03(2)}. Selected bond angles (°) for structure 1 {structure 2}. C10–C11–C12 179.1(3) {1.785(3)}; C11–C12–C13 175.0(3) {178.5(3)}; N2–H···O1 132(4)o {125(2)}; C_5H_4(cent)-Fe–C_5H_5(cent) 179.2 {179.3}.

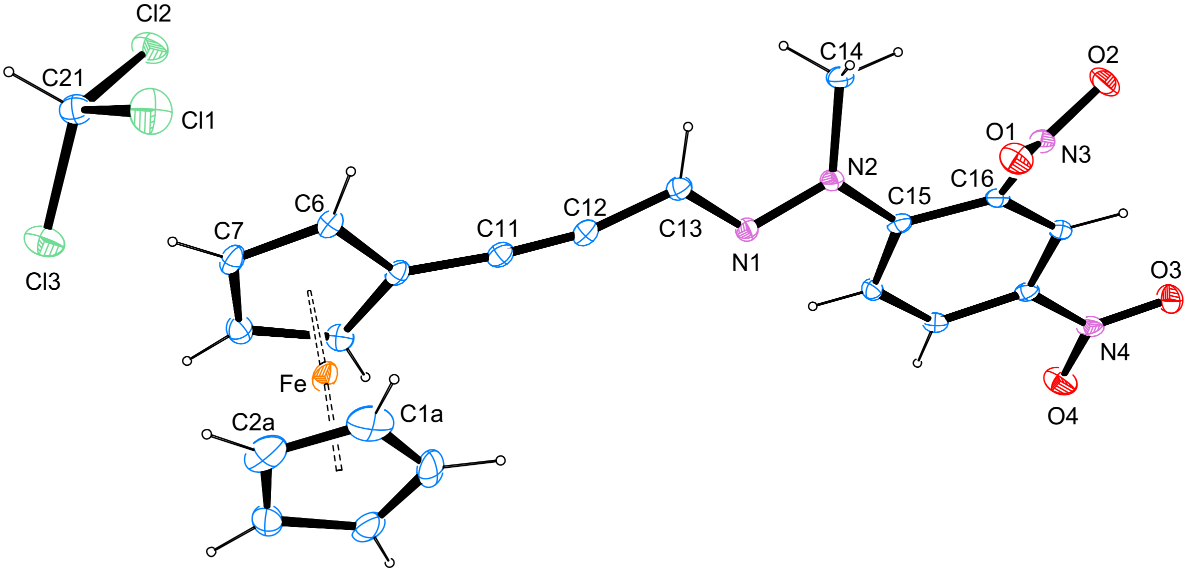

Fig. 7. Molecular structure and atom numbering for *anti*-[Fe(η^5-C_5H_5){η^5-C_5H_4–C≡C–CH=N–N(Me)$C_6H_3(NO_2)_2$-2,4}], *anti*-**7b**. Selected bond lengths (Å), Fe–C_5H_4(cent) 1.640; Fe–C_5H_5(cent) 1.649; C10–C11 1.420(3); C11–C12 1.203(3); C12–C13 1.420(3). Selected bond angles (°), C10–C11–C12 175.3(2); C11–C12–C13 168.7(2); C_5H_4(cent)–Fe–C_5H_5(cent) 174.4.

angles of 2.00(2) Å/132(4)° in **6a**, 1.91(4) Å/132(4)° in **6b** (structure 1) and 2.03(2) Å/125(2)° in **6b** (structure 2). These compare with 1.95(5) Å/144(2)° in *syn*-[Cb$^{\varphi}$–CH=N–N(H)$C_6H_3(NO_2)_2$-2,4] (structure 1) [12], 1.77(3) Å/130(3)° in *syn*-[Cb$^{\varphi}$–CH=N–N(H)$C_6H_3(NO_2)_2$-2,4] (structure 2) [12], and 1.96(2) Å/130(2)° in *anti*-[2-HOC_6H_4CH=N–N(H)$C_6H_3(NO_2)_2$-2,4] [54]. Bond lengths and angles within the C_5H_4–C≡C–CH=N–N(H)$C_6H_3(NO_2)_2$-2,4 moieties of **6a**, **6b** (structure 1) and **6b** (structure 2) are normal (c.f. *anti*-[2–HOC_6H_4CH=N–N(H)$C_6H_3(NO_2)_2$-2,4] [54]). Although the hydrazone group itself is relatively flat, particularly the dinitrophenyl component, it is not coplanar with the C_5H_4 ligand, and the additive effect of kinks in the multiple connecting atoms make comparisons with **4**/**5** difficult.

Replacement of the NH of the dinitrophenylhydrazone moiety of **6b** by NMe has many consequences. Only one isomer of **7b** appears to be formed (yield 80%) and in it the Fc–C≡C– and –N(H)$C_6H_3(NO_2)_2$–2,4 adopt the *anti*-conformation about C=N (Fig. 7). Unlike NH, NMe does not engage in hydrogen bonding to the *o*-N(3)O_2 group which, because of steric effects, is twisted and deflected away from the C_6H_3 plane. The N(2)–C–C–N(3) dihedral is 15.6° c.f. 2.4°/4.5°/0.6° in the NH hydrazones **6a**/**6b** (Structure 1)/(Structure 2). In contrast, the *p*-N(4)O_2 group is coplanar with the C_6H_3 ring. Despite the multiple connecting atoms the $C_5(H_4)$ and $C_6(H_3)$ planes are ca. parallel due to offset face-to-face (OFF) π–π interactions [55] within the crystal structure. An interaction between adjacent coplanar (0.3° dihedral) C_5H_5 and $C_6(H_3)$ rings generates

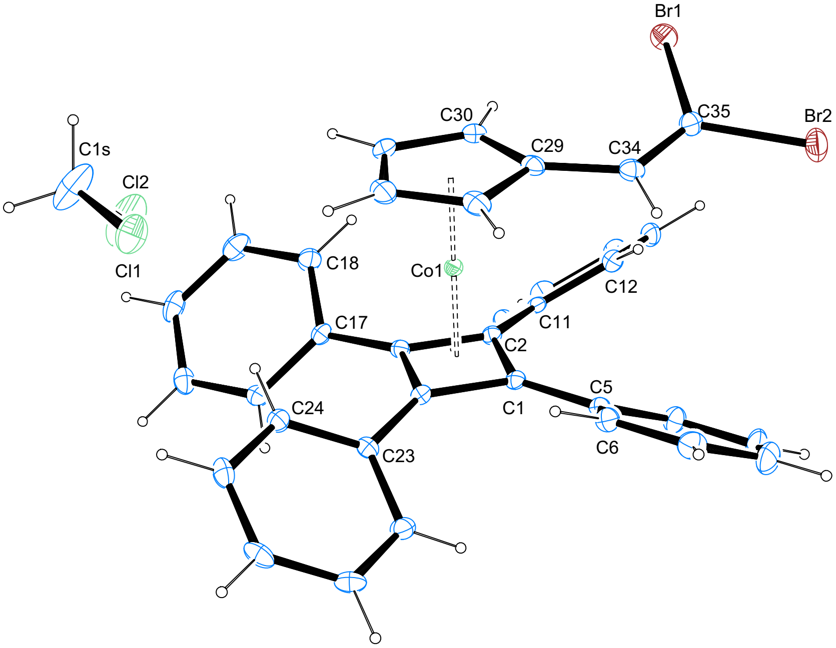

Fig. 8. Molecular structure and atom numbering for [Co(η^4-C_4Ph_4)(η^5-C_5H_4–CH=CBr_2)], **2a**. Selected bond lengths (Å), Co–C_5H_4(cent) 1.671; Co–C_4Ph_4(cent) 1.688; C29–C34 1.458(2); C34–C35 1.327(2). Selected bond angles (°), C29–C34–C35 129.8(1); C_5H_4(cent)–Co–C_4Ph_4(cent) 179.6.

inversion related dimers. The separation between C_5 and C_6 centroids is 3.77 Å. A second inversion related OFF interaction between C_5H_4 and $C_6(H)_3$ generates a ladder motif. In this case the angle between the rings is 2.8° and separation between C_5 and C_6 centroids is 3.63 Å. Although $\pi-\pi$ stacking is observed in **6a** and both forms of **6b**, the ladder motif and coplanarity between C_5 and C_6 rings is unique to **7b**.

The molecular structure has been determined of one of the reaction intermediates, $[Cb^{\varphi}-CH{=}CBr_2]$, **2a** (Fig. 8). As expected, it has approximately coplanar (1.2°) $C_4(Ph_4)$ and $C_5(H_4)$ ligands and the phenyl rings adopt the propeller configuration with tilt angles 28–39° from the C_4 plane. The $CH(34){=}CBr_2$ fragment is not coplanar with the $C_5(H_4)$ group to which it is bonded, but is tilted with respect to it by 20° so that the H34 lies below the C_5 plane i.e. is closer to Co with Co···H = 3.39 Å. This contrasts with the situation in $[Fe(\eta^5\text{-}C_5H_5)(\eta^5\text{-}C_5H_4-CH{=}CBr_2)]$, **2b**, where the $CH{=}CBr_2$ residue is tilted in the opposite sense by 12.9° so that the analogous H lies above the $C_5(H_4)$ plane (i.e. away from Fe) and the CBr_2 group below it [56].

3.3. Electrochemistry and spectroelectrochemistry

Electrochemical studies of the new $Cb^{\varphi}-$ and ferrocenyl compounds using cyclic voltammetry and differential pulse techniques were performed in dichloromethane solution. The results are presented in Table 2. Previous studies have shown $[Cb^{\varphi}-R]$ complexes undergo a one-electron, generally reversible oxidation at ca. 1 V (vs $[Fe(\eta^5\text{-}C_5Me_5)_2]^{+/0} = 0.00$ V) [10c, 12, 13, 17, 57]. The Cb^{φ} alkynes investigated here (**3a**–**7a**, **9a** and $[Cb^{\varphi}-C{\equiv}C-C_6H_5]$) display this couple. In all cases the oxidation appears to be chemically reversible with $i_{pc}/i_{pa} \cong 1$. A similar reversible one-electron oxidation is also observed for the ferrocenyl series of compounds, and in comparable derivatives the potential of the Cb^{φ} oxidation is consistently 330–350 mV anodic of the Fc redox couple. As might be expected, electron-withdrawing end-groups raise E° with respect to the Cb^{φ}- or Fc-terminal alkyne. Because the *E* and *Z* isomers of **9a** could not be separated, the E° reported in Table 2 is that of their 1:1 mixture. However, it is reasonable to believe that $E^\circ \approx 0.58$ and 1.06 V for both isomers provided that the electrochemical behaviour of **9a** is similar to that of its ferrocenyl counterpart **9b**, where E° (*E* isomer) $\approx E^\circ$ (*Z* isomer) and there is no evidence for *E*–*Z* isomerisation during cyclic voltammetry.

The 1e oxidation of Cb^{φ} in $[Cb^{\varphi}-C{\equiv}C-R]$ derivatives takes place at higher E° than those in $[Cb^{\varphi}-CH{=}CH-R]$ complexes, e.g. for $[Cb^{\varphi}-C{\equiv}C-C_6H_5]$ $E^\circ = 1.02$ V *vs.* 0.94/0.92 V for *E*/*Z*-$[Cb^{\varphi}-CH{=}CH-C_6H_5]$. Similar behaviour has been reported for $[Fc-C{\equiv}C-C_6H_5]$ ($E^\circ = 0.67$ V) *vs.* *E*-$[Fc-CH{=}CH-C_6H_5]$ (0.55 V) [9]. The first oxidation of *E*/*Z*-$[Cb^{\varphi}-C{\equiv}C-CH{=}CHFc]$, *Z*-$[Fc-C{\equiv}C-CH{=}CHFc]$ and *E*-$[Fc-C{\equiv}C-CH{=}CHFc]$ takes place at the *Fc*–CH=CH– moiety and at 0.58 V in all instances. The second oxidation occurs at the alkynyl metallocene, $Cb^{\varphi}-C{\equiv}C-$ or $Fc-C{\equiv}C-$ at 1.02 V or ca. 0.7 V respectively. These values do not differ greatly from those quoted above for $[Cb^{\varphi}-C{\equiv}C-C_6H_5]$ and $[Fc-C{\equiv}C-C_6H_5]$ which suggests that the first ferrocenyl oxidation has only a small effect on the oxidation potential of the second metallocenyl end-group.

One-electron oxidation of $[Cb^{\varphi}-C{\equiv}C-C_6H_5]$ in an OTTLE cell generates a new band in the UV–Visible spectrum at 575 nm associated with $\{Cb^{\varphi}\}^+$ and an additional low energy band in the near-IR spectral region centred at 960 nm. A similar feature has been observed in the OTTLE spectrum of $[Fc-C{\equiv}C-aryl]$ [9], $[Fc-CH{=}CH-aryl]$ [9] and $[Cb^{\varphi}-CH{=}CH-aryl]$ [13] systems, and is assigned to a ligand-to-metal charge transfer (LMCT) from the aryl to the $\{Fc\}^+$ or $\{Cb^{\varphi}\}^+$ centre. When aryl $=C_6H_5$ these have $\lambda_{max} = 797$ [9], 900 [9] and 955 [13] nm respectively. These observations strongly suggest that $\{Cb^{\varphi}\}^+$ is a better acceptor than $\{Fc\}^+$, and that the nature of the π-bridge ($C{\equiv}C$ *vs.* $CH{=}CH$) is also important for the latter but less so for the former.

The one-electron oxidation of the mixed ferrocenyl/Cb^{φ} compound **9a**, $[Cb^{\varphi}-C{\equiv}C-CH{=}CH\text{-}Fc]$ (*Z*/*E* mixture), was achieved by application of a 0.6 V anodic potential in the OTTLE cell. The resultant cation gives rise to an IVCT band at 1160 nm whereas the IVCT band of *E*-$[Cb^{\varphi}-CH{=}CH-Fc]^+$ is observed at 1290 nm [10c]. Thus, interpolation of the additional alkyne spacer attenuates the interaction between donor and acceptor. Insufficient separation between the $[\mathbf{9b}]^{+/0}$ and $[\mathbf{9b}]^{2+/+}$ oxidation potentials precluded a similar measurement for the bis-ferrocenyl yne-ene derivatives.

The absorption of **5b** at 565 nm is bleached upon oxidation in the OTTLE cell.

3.4. Bonding

Bonding in alkyne complexes of the general type $D-C{\equiv}C-CH{=}Y$ can be described as a hybrid of three mesomers *I*, *II* and *III* (Fig. 9)

Table 2
Electrochemical data.

		E°/V[a]		
		Fc oxidations		Cb^{φ} oxidation
3a	$[Cb^{\varphi}-C{\equiv}C-H]$[b]			1.05
4a	$[Cb^{\varphi}-C{\equiv}C-CHO]$			1.16
5a	$[Cb^{\varphi}-C{\equiv}C-CH{=}C(CN)_2]$			1.18
Syn–**6a**	*Syn*-$[Cb^{\varphi}-C{\equiv}C-CH{=}N-N(H)-C_6H_3(NO_2)_2-2,4]$			1.13
Anti–**7a**	*Anti*-$[Cb^{\varphi}-C{\equiv}C-CH{=}N-N(Me)-C_6H_3(NO_2)_2-2,4]$			1.06
E/*Z*–**9a**	*E*/*Z*–$[Cb^{\varphi}-C{\equiv}C-CH{=}CH-Fc]$	0.58		1.06
	$[Cb^{\varphi}-C{\equiv}C-C_6H_5]$ [19]			1.02
3b	$[Fc-C{\equiv}C-H]$ [9]	0.72		
4b	$[Fc-C{\equiv}C-CHO]$[c]	0.83		
5b	$[Fc-C{\equiv}C-CH{=}C(CN)_2]$	0.85		
Syn–**6b**	*Syn*-$[Fc-C{\equiv}C-CH{=}N-N(H)-C_6H_3(NO_2)_2-2,4]$	0.79		
Anti–**7b**	*Anti*-$[Fc-C{\equiv}C-CH{=}N-N(Me)-C_6H_3(NO_2)_2-2,4]$	0.71		
Z–**9b**	*Z*-$[Fc-C{\equiv}C-CH{=}CH-Fc]$	0.58	0.70	
E–**9b**	*E*-$[Fc-C{\equiv}C-CH{=}CH-Fc]$	0.58	0.68	
	$[Fc-C{\equiv}C-C_6H_5]$ [9]	0.67		

[a] Measured as 10^{-3} M in CH_2Cl_2/0.1 M $[Bu_4N][PF_6]$, Pt electrode. Referenced with internal decamethylferrocene reference, $[Fe(\eta^5\text{-}C_5Me_5)_2]^{+/0}$ 0.00 V, $[Fe(\eta^5\text{-}C_5H_5)_2]^{+/0} = 0.55$ V.

[b] Classen reports 1.09 V [17].

[c] Štěpnička reports 0.77 V [58].

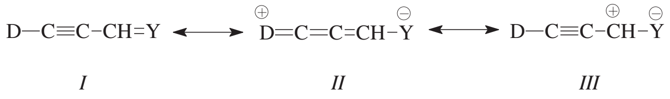

$$\underset{I}{\mathrm{D{-}C{\equiv}C{-}CH{=}Y}} \longleftrightarrow \underset{II}{\overset{\oplus}{\mathrm{D}}\mathrm{{=}C{=}C{=}CH{-}}\overset{\ominus}{\mathrm{Y}}} \longleftrightarrow \underset{III}{\mathrm{D{-}C{\equiv}C{-}}\overset{\oplus}{\mathrm{C}}\mathrm{H{-}}\overset{\ominus}{\mathrm{Y}}}$$

Fig. 9. The mesomers contributing to the bonding in D–C≡C–CH=Y complexes.

Both Cb^{φ} and Fc are relatively electron-rich donors with $Cb^{\varphi} <$ Fc by a small margin, and CH=Y within this work are acceptors of varying strengths. The stronger the acceptor the greater will be the contribution that mesomer *II* makes to any description of the bonding. This results in a lowering of the C≡C and C=Y bond orders which is most readily detected by spectroscopy. Thus ν(C≡C) stretching frequencies decrease for CH=Y = CH=NN(Me)$C_6H_3(NO_2)_2$-2,4 (**7a** 2207/**7b** 2205 cm^{-1}) > *anti*-CH=NN(H)$C_6H_3(NO_2)_2$-2,4 > CH=CH–Fc-*Z* and *E* > *syn*- CH=NN(H)$C_6H_3(NO_2)_2$-2,4 ≥ CHO > CH=C$(CN)_2$ » (–CH=CH–C_μ)(μ-CO)$(CO)_2Fe_2(\eta^5\text{-}C_5H_5)_2^+$ (**8a** 2148/**8b** 2147 cm^{-1}) indicating a decrease in the C≡C bond order along the series, though the consequences of ν(C≡C) and ν(C=Y) mixing must be borne in mind. The changes in C=Y bond order are less easy to detect, but can be seen when the ^1H NMR spectra of *E*-**9a**,**b** and [**8a**,**b**][BF_4] are compared. Both have CH=Y = *trans*–CH=CH–R, but in **9** R is the electron donor Fc/Cb^{φ} whilst in $[\mathbf{8}]^+$ it is the powerful acceptor group (–C_μ)(μ-CO)$(CO)_2Fe_2(\eta^5\text{-}C_5H_5)_2^+$. For both *E*-[**9**] J_{HH} = 16 Hz, the expected value for a normal alkene with a C–C bond order of 2 [38]. For [**8a**,**b**][BF_4] they are 14.2 Hz, consistent with a lower C=Y bond order, a larger contribution of *II* to the bonding in [**8a**,**b**] and increased D······Y π delocalization.

As the acceptor ability of CH=Y and the degree of delocalization within the D–C≡C–CH=Y molecules increase, the energy separation of HOMO and LUMO orbitals for the π system would be expected to decrease, and hence the wavelength of the lowest-energy electronic transition to increase as is observed.

In principle the C≡C bond length should increase as the degree of delocalization across it increases. In practice the crystallographically measured differences are random, small and within experimental error.

Various spectroscopic data show that there is poorer conjugation through C≡C than through C=C spacers. This is most clearly illustrated by comparing the spectra of [$Fe_2(\eta\text{-}C_5H_5)_2(CO)_2$(μ-CO)(μ-$C_\mu$–CH=CH–C≡C–Fc)][$BF_4$], [**8b**][$BF_4$], with that of [$Fe_2(\eta\text{-}C_5H_5)_2(CO)_2$(μ-CO)(μ-$C_\mu$–CH=CH–CH=CH–Fc)][$BF_4$]. The frequencies of the ν(CO) modes of the former (2033, 1996 sh, 1844 cm^{-1}) are higher than those of the latter (2027, 2001, 1837 cm^{-1}) and its C_μ has a higher δ (436 *vs.* 411). Both suggest that the donor effect of the Fc (and Cb^{φ}) group is less effective with a C≡C as opposed to a C=C spacer.

4. Conclusions

The series of [Cb^{φ}–C≡C–CH=Y] and [Fc–C≡C–CH=Y] complexes **4a**–**9a** and **4b**–**9b** show varying degrees of Donor–π–Acceptor behavior as measured by spectroscopic data (IR, NMR, UV/Vis). For the complexes with traditional acceptors, the acceptor strength follows the predicted order, with CHO < CH=C$(CN)_2$ < (–CH=CH–C_μ^+)(μ-CO)$(CO)_2Fe_2(\eta^5\text{-}C_5H_5)_2$. At the other terminus the ferrocenyl is a better donor than Cb^{φ}. Spectroscopic data also confirm that conjugation between donor and acceptor groups is poorer through C≡C than C=C π linking groups used in previous studies. X-ray crystallographic results provide no surprises, but illustrate the importance of intermolecular forces (and for the hydrazones intramolecular hydrogen bonding) in the solid state packing arrangement.

Acknowledgements

We thank the New Economy Research Fund (grant No.UOO-X0808) for support of this work (CJM & JS).

Appendix A. Supplementary material

CCDC 831403–831411 contain the supplementary crystallographic data for this paper. These data can be obtained free of charge from The Cambridge Crystallographic Data Centre via www.ccdc.cam.ac.uk/data_request/cif.

Appendix. Supplementary material

Supplementary material associated with this article can be found, in the online version, at doi:10.1016/j.jorganchem.2011.12.012.

References

[1] (a) J. Griffiths, Rev. Prog. Coloration 11 (1981) 37;
(b) G. Likhtenshtein, Stilbenes: Applications in Chemistry, Wiley-VCH Verlag GmbH & Co. KGaA, Weinheim, Germany, 2010;
(c) H. Meier, J. Gerold, H. Kolshorn, B. Mühling, Chem. Eur. J. 10 (2004) 360.

[2] (a) M.U. Winters, E. Dahlstedt, H.E. Blades, C.J. Wilson, M.J. Frampton, H.L. Anderson, B. Albinsson, J. Am. Chem. Soc. 129 (2007) 4291;
(b) T.L. Kinnibrugh, S. Salman, Y.A. Getmanenko, V. Coropceanu, W.W. Porter III, T.V. Timofeeva, A.J. Matzger, J.-L. Brédas, S.R. Marder, S. Barlow, Organometallics 28 (2009) 1350;
(c) Q.-Y. Cao, X. Lu, Z.-H. Li, L. Zhou, Z.-Y. Yang, J.-H. Liu, J. Organomet. Chem. 695 (2010) 1323.

[3] (a) M.I. Bruce, A. Burgun, C.R. Parker, B.W. Skelton, J. Organomet. Chem. 695 (2010) 619;
(b) P. Yuan, J. Yin, G. Yu, Q. Hu, S.H. Liu, Organometallics 26 (2007) 196.

[4] S.S. Malhotra, M.C. Whiting, J. Chem. Soc. (1960) 3812.

[5] C. Lo Sterzo, G. Bandoli, A. Dolmella, J. Chem. Soc. Dalton Trans. (1992) 697.

[6] (a) C.U. Pittman, L.R. Smith, J. Organomet. Chem. 90 (1975) 203;
(b) K. Wurst, O. Elsner, H. Schottenberger, Synlett (1995) 833;
(c) J.-G. Rodriguez, A. Oñate, R.M. Martin-Villamil, I. Fonseca, J. Organomet. Chem. 513 (1996) 71;
(d) M. Herberhold, Hong Yan, W. Milius, B. Wrackmeyer, J. Organomet. Chem. 623 (2001) 149;
(e) M. Bassetti, C. Pasquini, A. Raneri, D. Rosato, J. Org. Chem. 72 (2007) 4558.

[7] Á. Nievas, J.J. González, E. Hernández, E. Delgado, A. Martín, C.M. Casado, B. Alonso, Organometallics 30 (2011) 1920.

[8] A.J. Moore, A. Chesney, M.R. Bryce, A.S. Batsanov, J.F. Kelly, J.A.K. Howard, I.F. Perepichka, D.F. Perepichka, G. Meshulam, G. Berkovic, Z. Kotler, R. Mazor, V. Khodorkovsky, Eur. J. Org. Chem. (2001) 2671.

[9] L. Cuffe, R.D.A. Hudson, J.F. Gallagher, S. Jennings, C.J. McAdam, R.B.T. Connelly, A.R. Manning, B.H. Robinson, J. Simpson, Organometallics 24 (2005) 2051.

[10] (a) T. Farrell, T. Meyer-Friedrichsen, M. Malessa, D. Haase, W. Saak, I. Asselberghs, K. Wostyn, K. Clays, A. Persoons, J. Heck, A.R. Manning, J. Chem. Soc. Dalton Trans. (2001) 29;
(b) A.H. Flood, C.J. McAdam, K.C. Gordon, H.G. Kjaergaard, A.R. Manning, B.H. Robinson, J. Simpson, Polyhedron 26 (2007) 448;
(c) H.G. Kjaergaard, C.J. McAdam, A.R. Manning, H. Mueller-Bunz, P. O'Donohue, Y. Ortin, B.H. Robinson, J. Simpson, Inorg. Chim. Acta 361 (2008) 1616.

[11] Y. Ortin, J. Grealis, C. Scully, H. Müller-Bunz, A.R. Manning, M.J. McGlinchey, J. Organomet. Chem. 689 (2004) 4683.

[12] P. O'Donohue, C.J. McAdam, D. Courtney, Y. Ortin, H. Müller-Bunz, A.R. Manning, M.J. McGlinchey, J. Simpson, J. Organomet. Chem. 696 (2011) 1496.

[13] P. O'Donohue, C.J. McAdam, D. Courtney, Y. Ortin, H. Müller-Bunz, A.R. Manning, M.J. McGlinchey, J. Simpson, J. Organomet. Chem. 696 (2011) 1510.

[14] (a) J.F. Gallagher, P. Butler, R.D.A. Hudson, A.R. Manning, J. Chem. Soc. Dalton Trans. (2002) 75;
(b) C.J. McAdam, A.R. Manning, B.H. Robinson, J. Simpson, Inorg. Chim. Acta 358 (2005) 1673;
(c) P. Butler, J.F. Gallagher, A.R. Manning, H. Müller-Bunz, C.J. McAdam, J. Simpson, B.H. Robinson, J. Organomet. Chem. 690 (2005) 4545;
(d) P. Butler, A.R. Manning, C.J. McAdam, J. Simpson, J. Organomet. Chem. 693 (2008) 381.

[15] (a) T. Farrell, T. Meyer-Friedrichsen, J. Heck, A.R. Manning, Organometallics 19 (2000) 3410;
(b) T. Farrell, T. Meyer-Friedrichsen, M. Malessa, C. Wittenburg, J. Heck, A.R. Manning, J. Organomet. Chem. 625 (2000) 32;
(c) T. Farrell, T.C. Murphy, I. Asselberghs, T. Meyer-Friedrichsen, A. Persoons, J. Heck, A.R. Manning, Eur. J. Inorg. Chem. (2001) 2365;

(d) R.D.A. Hudson, I. Asselberghs, K. Clays, L.P. Cuffe, J.F. Gallagher, A.R. Manning, A. Persoons, K. Wostyn, J. Organomet. Chem. 637-639 (2001) 435.
[16] A.M. Stevens, C.J. Richards, Tetrahedron Lett. 38 (1997) 7805.
[17] J. Classen, R. Gleiter, F. Rominger, Eur. J. Inorg. Chem. 8 (2002) 2040.
[18] (a) H. Schimanke, R. Gleiter, Organometallics 17 (1998) 275;
(b) H.V. Nguyen, M.R. Yeamine, J. Amin, M. Motevalli, C.J. Richards, J. Organomet. Chem. 693 (2008) 3668.
[19] D. Courtney, A.R. Manning, C.J. McAdam, J. Simpson, Acta Cryst E67 (2011) m742–m743.
[20] (a) T.-Y. Dong, C.-P. Chen, C.-T. Kuo, S.-F. Lin, C.-N. Chen, S.-C. Hsu, Y.-S. Wen, Inorg. Chim. Acta 363 (2010) 1741;
(b) E. Champeil, S.M. Draper, J. Chem. Soc. Dalton Trans. (2001) 1440;
(c) K.-Q. Wu, J. Guo Yan, J.-F. Yan, L.-L. Xie, F.-B. Xu, S. Bai, P. Nockemann, Y.-F. Yuan, Organometallics 30 (2011) 3504;
(d) Á. Nievas, M. Medel, E. Hernández, E. Delgado, A. Martín, C.M. Casado, B. Alonso, Organometallics 29 (2010) 4291;
(e) P.J. Low, N.J. Brown, J. Clust. Sci. 21 (2010) 235;
(f) A.K. Diallo, C. Absalon, J. Ruiz, D. Astruc, J. Am. Chem. Soc. 133 (2011) 629.
[21] M. Rosenblum, A.K. Banerjee, N. Danieli, R.W. Fish, V. Schlatter, J. Am. Chem. Soc. 85 (1963) 316.
[22] P.L. Pauson, W.E. Watts, J. Chem. Soc. (1963) 2990.
[23] N.J. Lawrence, J. Liddle, D. Jackson, J. Chem. Soc. Perkin Trans. 1 (2002) 2260.
[24] A. Büldt, U. Karst, Analyt. Chem. 69 (1997) 3617.
[25] M. Nitay, W. Priester, M. Rosenblum, J. Am. Chem. Soc. 100 (1978) 3620.
[26] I. Noviandri, K.N. Brown, D.S. Fleming, P.T. Gulyas, P.A. Lay, A.F. Masters, L. Phillips, J. Phys. Chem. B. 103 (1999) 6713.
[27] SADABS, Bruker AXS Inc Madison, WI 53711 (2000).
[28] G.M. Sheldrick, Acta Cryst A64 (2008) 112.
[29] (a) P. McArdle, Appl. Cryst. 28 (1995) 65;
(b) C.F. Macrae, I.J. Bruno, J.A. Chisholm, P.R. Edgington, P. McCabe, E. Pidcock, L. Rodriguez-Monge, R. Taylor, J. van de Streek, P.A. Wood, J. Appl. Cryst. 41 (2008) 466.
[30] N. Suboya, R. Hamasaki, M. Ito, M. Mitsuishi, Y. Yamamoto, J. Mater.Chem. 13 (2003) 511.
[31] E.J. Corey, P.L. Fuchs, Tetrahedron Lett. 13 (1972) 3769.
[32] G. Doiseneau, G. Balavoine, T. Fillebeen-Khan, J. Organomet. Chem. 425 (1992) 113.
[33] E. Knoevenagel, Chem. Ber. 31 (1898) 2596.
[34] H.T. Openshaw, A Laboratory Manual of Qualitative Organic Analysis, second ed. Cambridge University Press, Cambridge, UK, 1951, p. 45.
[35] C.P. Casey, M.S. Konings, R.E. Palermo, R.E. Colborn, J. Am. Chem. Soc. 107 (1985) 5296.
[36] (a) G. Wittig, G. Geissler, Liebigs Ann. Chem. 580 (1953) 44;
(b) G. Wittig, U. Schöllkopf, Chem. Ber. 87 (1954) 1318.
[37] R.D. Stephens, C.E. Castro, J. Org. Chem. 28 (1963) 3313.
[38] R.M. Silverstein, G.C. Bassler, T.C. Morrill, Spectroscopic Identification of Organic Compounds, fourth ed. John Wiley & Sons, New York, 1981.
[39] J.C. Evans, R.A. Nyquist, Spectrochim. Acta 16 (1960) 918.
[40] G.W. King, S.P. So, J. Mol. Spec. 36 (1970) 468.
[41] E.A. Gastilovich, D.N. Shigorin, Russ. Chem. Rev. 42 (1973) 611.
[42] Spectral Database for Organic Compounds, SDBS, National Institute of Advanced Industrial Science and Technology (AIST), Japan, 2010.
[43] T. Steiner, M. Tam, A. Grzegorzewski, N. Schulte, N. Veldman, A.M.M. Schreurs, J.A. Kanters, J. Kroon, J. van der Maad, B. Lutz, J. Chem. Soc. Perkin Trans. 2 (1996) 2441.
[44] A.M. Asiri, Appl. Organomet. Chem. 15 (2001) 907.
[45] (a) S. Barlow, S.R. Marder, Chem. Commun. (2000) 1555;
(b) L. Rigamonti, B. Babgi, M.P. Cifuentes, R.L. Roberts, S. Petrie, R. Stranger, S. Righetto, A. Teshome, I. Asselberghs, K. Clays, M.G. Humphrey, Inorg. Chem. 48 (2009) 3562.
[46] Y.J. Jung, K.-I. Son, Y.E. Oh, D.-Y. Noh, Polyhedron 27 (2008) 861.
[47] (a) K. Schlögl, H. Egger, Leibigs Ann. Chem. 76 (1964) 76;
(b) K. Schlögl, H. Egger, Leibigs Ann. Chem. 76 (1964) 88.
[48] E. Stankovic, S. Toma, R. Van Boxel, I. Asselberghs, A. Persoons, J. Organomet. Chem. 637-639 (2001) 426.
[49] K.A. Walters, Y.-J. Kim, J.T. Hupp, Inorg. Chem. 41 (2002) 2909.
[50] S. Uchiyama, M. Ando, S. Aoyagi, J. Chromatogr. A 996 (2003) 95.
[51] J.D. Roberts, C. Green, J. Am. Chem. Soc. 68 (1946) 214.
[52] F.H. Allen, O. Kennard, D.G. Watson, L. Brammer, A.G. Orpen, R. Taylor, J. Chem. Soc. Perkin II (1987) S1.
[53] M. Zora, C. Açikgöz, T.A. Tumay, M. Odabaşoğlu, O. Büyüngör, Acta Cryst. C62 (2006) m327.
[54] H.H. Monfared, O. Pouralimardan, C. Janiak, Z. Naturforsch 62b (2007) 717.
[55] C. Janiak, J. Chem. Soc. Dalton Trans. (2000) 3885.
[56] S. Clément, L. Guyard, M. Knorr, F. Villafañe, C. Strohmann, M. Kubicki, Eur. J. Inorg. Chem. (2007) 5052.
[57] U. Koelle, Inorg. Chim. Acta 47 (1981) 13.
[58] P. Štěpnička, L. Trojan, J. Kubišta, J. Ludvík, J. Organomet. Chem. 637-639 (2001) 291.